



Contents lists available at ScienceDirect

Arabian Journal of Chemistry

journal homepage: www.ksu.edu.sa

Original article

Cassia fistula leaves extract profiling and its emphasis on induced ulcerative colitis in male rats through inhibition of caspase 3 and cyclooxygenase-2

Nada A. Abdellatif^{a,1}, Enas E. Eltamany^{a,1}, Nahla S. El-Shenawy^b, Mohamed S. Nafie^c,
Yasmin M. Hassan^d, Rasha A. Al-Eisa^e, Jihan M. Badr^{a,*}, Reda F.A. Abdelhameed^{a,f}

^a Department of Pharmacognosy, Faculty of Pharmacy, Suez Canal University, Ismailia 41522, Egypt

^b Department of Zoology, Faculty of Science, Suez Canal University, Ismailia 41522, Egypt

^c Department of Chemistry (Biochemistry program), Faculty of Science, Suez Canal University, Ismailia 41522, Egypt

^d Department of Botany and Microbiology, Faculty of Science, Suez Canal University, Ismailia 41522, Egypt

^e Department of Biology, Collage of Science, Taif University, Taif 21944, Saudi Arabia

^f Department of Pharmacognosy, Faculty of Pharmacy, Galala University, New Galala 43713, Egypt



ARTICLE INFO

Keywords:

C. fistula
Antioxidant
TFC
TPC
LC/MS/MS
ulcerative colitis
COX-2
caspase-3
in silico

ABSTRACT

The objective of the study was to determine the total phenolic and total flavonoid contents (TPC and TFC, respectively), as well as the solvent-partitioned fractions, of the leaf extract of *Cassia fistula*. Using DPPH, TAC, and FRAP tests, the *in vitro* antioxidant properties of crude extract and its ethyl acetate fraction were investigated. Additionally, *C. fistula* chemical profiling was accomplished using LC-ESI-MS/MS. Along with that, the effectiveness of crude extract (200 and 400 mg/kg) in treating male rats with ulcerative colitis (UC) induced by acetic acid was assessed. According to the findings, the ethyl acetate fraction had the highest concentrations of TPC (12.36 1.46 mg GAE/100 mg) and TFC (5.12 0.64 mg QE/100 mg), as well as impressive *in vitro* antioxidant activity with IC₅₀ values of DPPH (12.7 g/mL), FRAP (4.87 0.71 mM Fe+2/g), and TAC (55. Fifty-five chemicals, predominantly phenolics (catechins, flavonoids, anthraquinones, chalcones, and phenolic acids), were detected by the LC/MS/MS. The anti-UC effect of *C. fistula* was dose-dependent. The hematological parameters, liver biomarkers, oxidative stress, histopathology, and immunohistochemistry revealed that prophylactic administration of crude extract to colitis rats ameliorated all the previous biomarkers. However, when the crude extract was administered on established colitis, it facilitated the recovery of the inflamed mucosa and showed better results than the protection mode. The phytoconstituents of *C. fistula* that were discovered here by LC/MS/MS were examined by molecular docking studies for their binding affinities towards COX-2 and caspase-3 proteins to highlight the anti-inflammatory and antiapoptotic activities of the plant. The Emodin compound displayed the highest binding affinity for COX-2 proteins, while isorhamnetin was discovered to have the best binding associations with the essential amino acids of caspase-3. Procyanidin B2 interestingly shows potent interactions with important amino acids of two targets. This study has made it possible to utilize *C. fistula* in the treatment of UC and has clarified its mechanism of action.

1. Introduction

Inflammation is a natural physiological process that occurs in response to tissue injury, infection, and a variety of other conditions that contribute to pathological changes (Kwon et al., 2005). Inflammatory bowel diseases (IBD) are divided into two types: UC and Crohn's disease, both of which are marked by epithelial ulceration. It can lower the quality of life of patients and increase the risk of colon cancer (Abraham

et al., 2017). Inflammatory Bowel Disease (IBD) is a condition with an unknown definitive cause, but it is widely accepted that various factors such as environmental, microbial, genetic, and immunogenic elements interact to trigger the mucosal T-cell immune response. This immune response leads to the release of inflammatory mediators, including reactive nitrogen species (RNS) and reactive oxygen species (ROS). The consequences of this immune activation include cell infiltrations, a breakdown of the mucosal barrier, a decrease in antioxidant enzymes in

* Corresponding author.

E-mail address: gehan_ibrahim@pharm.suez.edu.eg (J.M. Badr).

¹ Equal contribution

<https://doi.org/10.1016/j.arabjc.2024.105672>

Received 28 November 2023; Accepted 8 February 2024

Available online 16 February 2024

1878-5352/© 2024 The Author(s). Published by Elsevier B.V. on behalf of King Saud University. This is an open access article under the CC BY-NC-ND license (<http://creativecommons.org/licenses/by-nc-nd/4.0/>).

the colonic mucosa, the production of anti-inflammatory cytokines, and the activation of nuclear factor kappa-light-chain-enhancer of activated B cells (NF- κ B). Ultimately, these processes contribute to apoptotic injuries in the colon (Shahid et al., 2022).

Most patients with IBD who require ongoing treatment to keep the disease under control find that the existing medications are far from satisfactory. Furthermore, many of the currently synthetic drugs, such as aminosalicylates, corticosteroids, immune modulators, and biological treatments, have a range of adverse effects with varying reactions that can deteriorate over time as well as limit their clinical efficacy. Nearly 50% of IBD patients are dissatisfied with the current IBD treatments, which is why plant-based drugs are growing in popularity. This is due to their pharmacological traits, which also aid in addressing nutritional shortages, decreasing oxidative stress and inflammation, and preventing unforeseen negative effects (Bastaki et al., 2022). Chromatography, microscopy, and other research techniques, as well as phytochemical, pharmacological, and allied approaches, are the principal techniques utilized to evaluate these drugs (Sharma, 2021).

Nearly all medicinal plants are composed of phenolic compounds, particularly flavonoids, which are powerful bioactive substances. Plants from the Acacia species (Fabaceae Family) are abundant in phenolic compounds, flavonoids, and tannins and can be used in various medical conditions (Abdallah et al., 2020). *Cassia fistula* (*C. fistula*) Linn is a particular plant belonging to the family Fabaceae that has great ethnomedicinal significance and is widely used in Unani and Ayurvedic medicines and holds a prominent place in traditional medicine. Renowned for its efficacy against various ailments, including skin diseases, liver issues, tuberculous glands, and more, the plant has been suggested for treating conditions like haematemesis, pruritus, leucoderma, and diabetes. Traditional methods of administration include infusions, decoctions, or powders. The plant's versatile applications highlight its significance in traditional healing practices (Ali, 2014). It originated in India and Sri Lanka and has since expanded to several locations, including Mexico, China, East and South Africa (Sanoria et al., 2020). *C. fistula* confirmed the therapeutic effects and its role in the management of health via modification of biological processes due to its high antioxidant content. Some outcomes based on animal models have shown the safety and effectiveness of medications, opening up new avenues for the treatment of human illness and assisting in disease prevention (Rahmani, 2015). The generation of ulcerative colitis (UC) through acetic acid (AA) has led to extensive exploration of chemical-induced animal models of colonic inflammation. These models aim to comprehend the underlying pathophysiological mechanisms of UC and evaluate the effectiveness of treatment medications (Dothel et al., 2013, Zabihi et al., 2024).

The antioxidant properties of *C. fistula* leaves have been reported (Khan et al., 2012; Kaur et al., 2020). The plant has been found to possess antioxidant, antimicrobial, anti-inflammatory, antidiabetic, antitumor, and hepatoprotective activities, among others. Pharmacological reviews on medicinal plants highlight the significance of *C. fistula* in providing valuable bioactive natural products. The exploration of these properties opens avenues for developing novel pharmaceutical products with potential therapeutic benefits. *C. fistula*'s multifaceted pharmacological profile underscores its importance in the search for new and effective medicinal compounds (Mwangi et al., 2021). The current study focused on investigating the antioxidant potential of *C. fistula* leaves, considering their traditional significance. Additionally, the study explored the total phenolic and flavonoid content in different extracts of *C. fistula* leaves. The research also evaluated the leaves' potential protective and treatment effects against ulcerative colitis induced by acetic acid. Furthermore, the study involved molecular docking of the identified compounds against protein structures of caspase-3 and cyclooxygenase-2 (COX-2) using Auto Dock Vina software.

2. Materials and Methods

2.1. Chemicals and reagents

Chloroform (99.50%), ethyl acetate (99.90%), butanol (99.7%), methanol (99.8%), *n*. hexane (99.0%), silica gel, TLC plates, and acetic acid (AA, 99.8%) were obtained from Alpha Chemika (India). Sulfasalazine was brought from KAHIRA PHARM & CHEM (Cairo, Egypt). The highest purity and analytical grade were used for all other chemicals. Spectrophotometric of colonic tissue for the determination of malondialdehyde (MDA), catalase (CAT), glutathione peroxidase (GPx), superoxide dismutase (SOD), reduced glutathione (GSH), cyclooxygenase-2 (COX-2) and caspase-3 were purchased from Biodiagnostic Co. (Giza, Egypt).

2.2. Plant material and sample preparation

Fresh leaves of *C. fistula*, Fabaceae (Leguminosae) were collected in March from Suez Canal University, Ismailia, Egypt. Dr. Yasmien Mohamed Hassan of the Department of Botany at Suez Canal University's Faculty of Science verified the authenticity of the plant. For future use, a specimen voucher was kept in the lab [202005 M1].

For seven days, the plant material was allowed to air dry. Using a heavy-duty blender, seven kilograms of the dried material were ground into a fine powder, yielding (3.5 kg). A greenish-black residue weighing 660 g was obtained by macerating fine powder with 3 \times 8 L of methanol, filtering, and concentrating the solution in a rotary evaporator at 40 $^{\circ}$ C. After allowing the residue to dry, fractionation of the crude extract involved suspending 290 g in 200 mL of distilled water and partitioning with *n*-hexane (Hex). The resulting aqueous layer was concentrated and sequentially partitioned with chloroform (CHCl₃), ethyl acetate (EtOAc), and *n*-butanol (*n*-BuOH) (Khurm et al., 2021). Vacuum concentration of these solvent extracts yielded fractions of *n*-hexane, CHCl₃, EtOAc, and *n*-butanol, weighing 128.4 g, 10.18 g, 63.24 g, and 79.59 g, respectively.

2.3. Assessment of total phenolic and flavonoids

The total phenolic content (TPC) of both crude and fractional extracts of *C. fistula* was determined using spectrophotometry, following the protocol outlined by Singleton and Rossi (1965). The Folin-Ciocalteu method was employed for the TPC assay, and the results were quantified and presented as mg gallic acid equivalents (GAE) per gram of extract. Additionally, the total flavonoid content (TFC) was assessed using the method described by Djeridane et al. (2020), with TFC results expressed as mg quercetin equivalents (QE) per gram of extract.

2.4. In vitro antioxidant activity of crude extract and its EtOAc fraction

The DPPH free radical scavenging, FRAP, and TAC tests were employed in triplicate by the Regional Centre for Mycology and Biotechnology (RCMB) at Al-Azhar University to assess the antioxidant properties of crude extract and its EtOAc fraction.

2.4.1. DPPH free radical scavenging activity

Measurements were also made of the absorbance of the reference compound ascorbic acid and the DPPH radical without antioxidant (control) (Obob, 2005). Every calculation was made in three duplicates and averaged. The following formula was used to determine the DPPH radical's percentage inhibition (PI):

$$PI = \left\{ \frac{(AC - AT)}{AC} \right\} \times 100 \quad (1)$$

Where AC = Absorbance of the control at t = 0 min and AT = absorbance of the sample + DPPH at t = 16 min (Yen and Duh, 1994).

Table 1

Total phenolic contents (TPC) and total flavonoid contents (TFC) of *C. fistula* crude extract and fractions.

Sample	Total Flavonoids (mg QE)/ 100 mg)	Total Phenolic (mg GAE)/ 100 mg)
<i>C. fistula</i> crude extract	4.25 ± 0.71	10.56 ± 1.32
<i>n</i> -Hexane fraction	1.04 ± 0.32	3.22 ± 0.94
CHCl ₃ fraction	3.89 ± 0.63	9.48 ± 1.72
EtOAc fraction	5.12 ± 0.64	12.36 ± 1.46
<i>n</i> -BuOH fraction	5.03 ± 0.94	11.47 ± 1.29

TPC is expressed as mg gallic acid equivalents (GAE)/g extract and TFC is expressed as mg quercetin equivalents (QE)/g extract. Data are presented as mean ± S.D (n = 5).

Table 2

In vitro antioxidant activity *C. fistula* extract and its EtOAc fraction.

Samples	TAC (mg GAE/ g)	FRAP (mMol Fe ⁺² / g)	DPPH IC ₅₀ (µg/ mL)
Crude extract	48.37 ± 3.19	2.76 ± 0.38	60.6
EtOAc fraction	65.19 ± 5.33	4.87 ± 0.71	12.7
BHT	76.43 ± 3.89	6.98 ± 0.76	–
Ascorbic acid	–	–	10.6

Data are presented as mean ± S.D (n = 3). TAC: total antioxidant capacity, FRAP: ferric antioxidant power, and BHT: butylated hydroxytoluene

The study utilized the 50 % inhibitory concentration (IC₅₀) and graphical representations of the dose–response curve to determine the concentration required to inhibit the (DPPH) radical by 50 %. This approach allowed for the assessment of the effectiveness of the tested compounds in scavenging the DPPH radical.

2.4.2. Ferric reducing antioxidant power (FRAP)

The formula for the (FRAP) of the methanol extract was derived following the method outlined by Nsimba et al. (2008). The reaction progress was tracked by measuring the absorbance change at 593 nm using the Milton Roy Spectronic 1201 spectrophotometer in Houston, Texas, USA. This approach allowed for the quantification of the antioxidant power of the methanol extract.

2.4.3. Total antioxidant capacity (TAC)

The extract TAC was assessed utilizing a phospho-molybdenum test and spectrophotometric analysis. With a few adjustments, the technique was carried out as Saeed et al. (2012) had previously reported. Milton Roy, Spectronic 1201, Houston, TX, USA was used to measure the absorbance using a UV–visible spectrophotometer at 695 nm against a blank sample. Gallic acid equivalents were calculated from the TAC values (mg/g of dry material). The reference substance was butylated hydroxytoluene (BHT; Sigma-Aldrich, St. Louis, MO, USA).

2.5. LC-ESI-TOF-MS/MS analysis of *C. fistula* crude extract

LC-ESI-TOF-MS/MS (SCIEX, Santa Clara, CA, USA) was used to investigate the nature and diversity of *C. fistula* phytochemicals. The samples were prepared as described before (Eltamany et al., 2020; Eltamany et al., 2022; Goda et al., 2022; Anlas et al., 2023), deionized H₂O, CH₃CN, and MeOH were combined in the mobile phase working solution in a 50/25/25 ratio. One mL of MP-WS was mixed with 50 mg of weighted dry extract before being vortexed for two min. Following that, 10 min of ultrasonication and 10 min of 10,000 rpm centrifugation were completed. The produced solution was withdrawn, and a further 50 L aliquot was diluted with the reconstitution solvent. A 2.5 g/L solution was prepared and injected in both negative and positive modes using 25 mL. A blank sample with 25 L of mobile phase working solution

was also injected. In positive TOF MS mode, (A) 5 mM NH₄COOH buffer (pH = 3) with 1 % MeOH was used; in negative TOF MS mode, (B) 5 mM NH₄COOH (pH = 8) with 1 % methanol was used; and for both modes, (C) mobile phase consisting of 100 % CH₃CN was used. The pre-column had in-line filter discs (Phenomenex, 0.5 m X 3.0 mm), and the column was an X-select HSS T3 (Waters, 2.5 m, 2.1 X 150 mm), with a flow rate of 0.3 mL/min. The column operated at a temperature of 40 °C, with an injection volume of 10 µL.

Data processing utilized MS-DIAL3.52ur and Master View software, with peak extraction criteria: Sample-to-blank feature intensities greater than 5 and a Signal-to-Noise ratio of at least 5 for non-targeted analysis. Compound identification relied on precise mass measurements (*m/z*), MS/MS data, spectrum library exploration, and comparisons with public repositories (MassBank NORMAN, MassBank MoNA, PubChem, xxx) and literature retention periods. (Hu et al., 2023)

2.6. In vivo study

2.6.1. Experimental and Animal Ethics

Three hundred and fifty male albino rats weighing between one hundred and two hundred grams were acquired at the age of ten weeks from the Egyptian Organisation for Biological Products and Vaccines located in Cairo, Egypt. The rats were acclimatized for ten days under controlled conditions of 25 ± 3 °C, with a regular light/dark cycle, and were provided with unrestricted access to water and laboratory meal pellets during this period. All experimental procedures were approved and performed in compliance with the guide lines of the Research Ethical Committee of the Faculty of Pharmacy, Suez Canal University (Approval No. 202005 M1).

2.6.2. Induction of Ulcerative Colitis and Treated Groups

After a 24-hour fast with unrestricted access to water, the animals' stomach contents were emptied. The procedure that Hagar et al. (2007) had previously outlined was used to produce colitis. An intraperitoneal injection of KX rat cocktail (0.1 mL/100 g rat weight) was used to sedate each rat. includes 9.1 mg/kg of xylazine and 91 mg/kg of ketamine. A 2 mm diameter polyurethane enteral feeding tube was placed to a depth of 4.5 cm, and 2 mL of 3 % AA was injected into the rectum through it. The rats were kept in the Trendelenburg position during reinstallations and for a minute after stollations to stop solution leakage. The rats' diarrhea or rectal bleeding after 24 h suggested that colitis had been induced (Alsharif et al., 2022) *C. fistula* extract of doses (200 and 400 mg/kg) (Bhakta et al., 1999) were dissolved in 0.1 % DMSO and administered orally to the rats as indicated in the following groups.

Seven groups of five rats each were used in this experimental study, and they were split randomly as follows:

Group I: For 17 days, 0.1 % dimethyl sulfoxide (DMSO) was administered transrectally to the control group.

Group II: Colitis group, in which 14 days of 0.1 % DMSO transrectally were administered after 3 days of no therapy to produce ulcerative colitis (UC).

Group III: After transrectally administering AA for three days straight to induce colitis, 500 mg/kg (Owusu et al., 2020) of sulfasalazine medication for body weight was given for 14 days.

Group IV: Following UC induction, MLE 200 mg/kg of body weight was administered for 14 days.

Group V: Following UC induction, MLE 400 mg/kg of body weight was administered for 14 days.

Group VI: UC was induced after 14 days of MLE 200 mg/kg of body weight being given as a protective dose.

Group VII: UC was produced after 14 days of MLE 400 mg/kg of body weight being given as a protective dose.

2.6.3. Determination of body weight, and macroscopic scores

The body weight of each animal was measured at the start of the

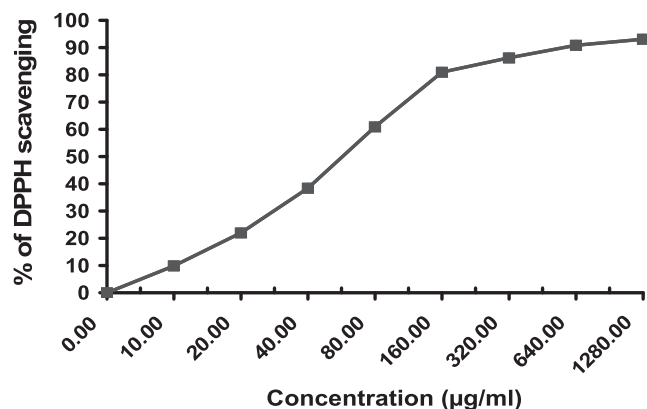


Fig. 1. Dose-dependent DPPH free radical scavenging of crude extract.

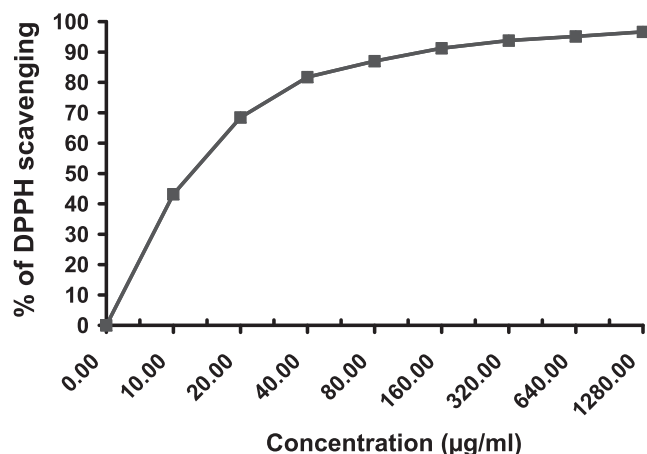


Fig. 2. Dose-dependent DPPH free radical scavenging of ethyl acetate fraction.

experiment and again after 21 days for every group. The colon's weight after the trial was assessed, as was the colon's weight-to-length ratio.

Macroscopic inflammation scores were assigned based on clinical features of the colon using an arbitrary scale ranging from 0 to 4 as follows: 0 (no macroscopic changes), 1 (mucosal erythema only), 2 (mild mucosal edema, slight bleeding or small erosions), 3 (moderate edema, slight bleeding ulcers or erosions), 4 (severe ulceration, edema, and tissue necrosis) (Salama et al., 2020).

Stool consistency was assessed with the following scoring criteria: 0 for normal, 1 and 2 for loose stool, and 3 and 4 for diarrhea.

2.6.4. Collection of blood and tissue

Blood samples were swiftly collected from the medial retro-orbital venous plexus of starved rats under anesthesia, using capillary tubes (Micro Hematocrit Capillaries, Mucaps) (El-Shenawy et al., 2006). The collected blood was processed to extract serum, which was then centrifuged for 15 min at 4000 rpm to assess liver biomarkers. Additional blood collected in tubes containing EDTA was reserved for hematological analysis.

A suitable colonic slice was completed after adipose tissue was removed and a cool, normal saline rinse was administered. Colon homogenates were extracted from the remaining sections and stored for biochemical research at 80 °C. Colonic segments including the third section were preserved in 10 % neutral buffered formalin for further histological and immunohistochemical examination.

2.6.5. Hematological evaluation

Cell counts were conducted using the Humalog System Analyzer, providing data on white blood cells (WBCs), red blood cells (RBCs),

platelets count, hemoglobin (HGB), hematocrit (HCT), mean cell volume (MCV), mean cell hemoglobin (MCH), and mean cell hemoglobin concentration (MCHC). The measurement included the number of WBCs per cubic milliliter of blood, and WBC differentiation was also assessed.

2.6.6. Liver biomarker evaluation

Serum activities of aspartate transaminase (AST), alanine transaminase (ALT), and alkaline phosphatase (ALP) were assessed using kits from Sentinel Diagnostics (Milan, Italy). Additionally, total bilirubin and protein levels were determined through spectrophotometry with commercial kits from Boehringer Mannheim GmbH (Mannheim, Germany). In the protein assay, the reaction with copper in the biuret reagent led to an increase in absorbance at an alkaline pH. The resulting rise in absorbance at 550 nm, attributed to the formation of a colored complex, was directly proportional to the concentration of protein in the reaction (Gornall, 1949).

2.6.7. Assessment of oxidative stress and antioxidants

Malondialdehyde (MDA) a marker of lipid peroxidation (LPO) in mucosal tissue induced by reactive oxygen species was measured in serum by the thiobarbituric acid assay (TBA) as previously described by Ahmed and Zaki (2009).

In addition, serum antioxidant defense enzymes that counteract the oxidative stress in colonic tissues were estimated. Superoxide dismutase (SOD) was determined according to Nishikimi et al. (1972). Catalase (CAT) was responsible for the conversion of H₂O₂ into H₂O and was measured as outlined in Aebi (1984). Glutathione peroxidase (GPx) was determined as previously mentioned by Paglia and Valentine (1967). Reduced glutathione (GSH) levels were estimated based on the method of Beutler et al. (1969), who reported that the 5,5'-dithiobis- (2-nitrobenzoic acid) is reduced by the SH group to form 1 mol of 2-nitro-5-mercaptobenzoic acid per mole of SH. Finally, serum total antioxidant capacity was evaluated following the method described (Han et al., 2012).

2.6.8. Histopathological study

The collected colon tissues were preserved for 24 h in 10 % neutral buffered formalin, followed by a tap water wash, dehydration, and xylene clearance. The samples were then regularly prepared to yield paraffin-embedded slices that were 5–7 µm thick, and they were then stained with H&E stain for light microscopy analysis (Nagahashi et al., 2017).

2.6.9. Immunohistochemical (IHC) evaluation of cyclooxygenase-2 (COX-2) and caspase-3

In colonic tissues, the activity of COX-2 (an inflammatory marker) and Caspase-3 (a marker for apoptosis) was determined by IHC. Sections from colon tissues were prepared and stained with anti-caspase 3 (Catalog number GTX30246, GeneTex, Irvine, CA, USA) and anti-COX-2 (Catalog number ab16701, Abcam, Cambridge, UK.) and after preparation according to the methods mentioned (Chang et al., 2019; Eltamany et al., 2021), respectively. The immunoreaction was visualized using 3,3'-diaminobenzidine (Power-Stain™ 1.0 Poly HRP DAB Kit for Mouse + Rabbit, GENEMED, South San Francisco, CA, USA) as a chromogen, with Mayer's hematoxylin used as a counterstain. Selected portions of the colon were captured with a digital camera (Olympus Dp25). Quantification of COX-2 and Caspase-3 reactivity was performed through image analysis software (ImageJ version 1.53 h). The results were expressed as the mean area of immunopositive cells (IHC) per mm², calculated using a specific equation:

$$\% \text{IHC stained area} = \text{IHC stained area} / \text{total area} \times 100$$

2.7. Molecular docking

Molecular modeling investigations were conducted using Chimera-

Table 3
Metabolites identified in *C. fistula* crude extract using LC-ESI/TOF/MS/MS.

Compound No.	Rt (min)	Proposed compound	Molecular formula	Precursor type	Obs. m/z for Precursor	Calcd. m/z for Precursor	Mass error	MS/MS	Ref.
Catechins and procyanidins									
1.	4.645	Procyanidin B2	C ₃₀ H ₂₆ O ₁₂	[M-H] ⁻	577.1353	577.1346	1.2129	577,451,425,407,289	(Kusumaningtyas, 2020; Elmongy et al., 2022)
2.	4.919	Procyanidin B1	C ₃₀ H ₂₆ O ₁₂	[M-H] ⁻	577.1381	577.1346	6.0644	577,425,289	(Elmongy et al., 2022)
3.	5.478	Epicatechin	C ₁₅ H ₁₄ O ₆	[M-H] ⁻	289.0703	289.0712	-3.1134	289,123,161,203,245	(Goufo et al., 2020; Abdelhameed et al., 2021)
Flavones, Flavonols and flavanones									
4.	2.741	Eriodictyol-7-O-glucoside	C ₂₁ H ₂₂ O ₁₁	[M-H] ⁻	449.1100	449.1084	3.5626	449,287,269,259	(Negm et al., 2022b)
5.	4.932	Luteolin-3', 7-di-O-glucoside	C ₂₇ H ₃₀ O ₁₆	[M-H] ⁻	609.1421	609.1456	-5.7458	609,563,447,285	(Abbas et al., 2022)
6.	5.071	Quercetin-3,4'-O-di-β-glucopyranoside	C ₂₇ H ₃₀ O ₁₇	[M-H] ⁻	625.143	625.1405	3.9991	625,463,301	(Attallah et al., 2021)
7.	5.557	Kaempferol-7-neohesperidoside	C ₂₇ H ₃₀ O ₁₅	[M-H] ⁻	593.1591	593.1506	14.3303	593,285	(Abdelhameed et al., 2021; Abbas et al., 2022)
8.	5.795	Kaempferol-3-O-robinoside-7-O-rhamnoside	C ₃₃ H ₄₀ O ₁₉	[M-H] ⁻	739.2134	739.2086	6.4934	739,575,285,284,179	(Abd Ghafar et al., 2018; Thabit et al., 2018)
9.	5.821	Rutin	C ₂₇ H ₃₀ O ₁₆	[M + H] ⁺	611.1655	611.1612	7.0358	611,465,303	(Attallah et al., 2021)
10.	6.713	Vitexin	C ₂₁ H ₂₀ O ₁₀	[M + H] ⁺	433.1151	433.1135	3.6942	433,397,313,283,271	(Abbas et al., 2022)
11.	6.784	Taxifolin	C ₁₅ H ₁₂ O ₇	[M-H] ⁻	303.0512	303.0505	2.3098	303,285,151	(Sun et al., 2007; Chen et al., 2020)
12.	6.9785	Quercitrin	C ₂₁ H ₂₀ O ₁₁	[M-H] ⁻	447.0938	447.0927	2.4603	447,284,301	(Wang et al., 2013; Eltamany et al., 2022)
13.	7.408	Isorhamnetin-3-O-glucoside	C ₂₂ H ₂₂ O ₁₂	[M-H] ⁻	477.1045	477.1033	2.5152	447,315,300	(Brito et al., 2014; Abbas et al., 2022)
14.	7.492	Naringenin-7-O-glucoside	C ₂₁ H ₂₂ O ₁₀	[M-H] ⁻	433.1139	433.1135	0.9235	433,271,256	(Attallah et al., 2021; Elmongy et al., 2022; Negm et al., 2022b)
15.	7.617	Myricetin	C ₁₅ H ₁₀ O ₈	[M-H] ⁻	317.03	317.0297	0.9463	137, 151,179, 289, 317	(Pereira et al., 2017)
16.	7.691	Diosmin	C ₂₈ H ₃₂ O ₁₅	[M + H] ⁺	609.1779	609.1819	-6.5662	609,301,286	(Chou et al., 2021; Abbas et al., 2022)
17.	7.781	Kaempferol-3-O-rhamnoside	C ₂₁ H ₂₀ O ₁₀	[M-H] ⁻	431.0995	431.0978	3.9434	431,285,255,151	(Abbas et al., 2022), Abo-Elghiet et al., 2022)
18.	8.369	Eriodictyol	C ₁₅ H ₁₂ O ₆	[M-H] ⁻	287.0564	287.0556	2.7869	135,151,287	(Brito et al., 2014; Abdelhameed et al., 2021)
19.	9.007	Luteolin	C ₁₅ H ₁₀ O ₆	[M-H] ⁻	285.0406	285.0399	2.4558	285,133	(Elhady et al., 2022; Goda et al., 2022)
20.	9.271	Quercetin	C ₁₅ H ₁₀ O ₇	[M-H] ⁻	301.0354	301.0348	1.9931	301,283,151	(Brito et al., 2014; Chen et al., 2020)
21.	9.631	Isorhamnetin	C ₁₆ H ₁₂ O ₇	[M-H] ⁻	315.0515	315.0505	3.1741	317,151,243,271,300	(Lin et al., 2013; Goda et al., 2022)
22.	9.733	Kaempferol	C ₁₅ H ₁₀ O ₆	[M + H] ⁺	287.0572	287.0556	5.57	278, 269, 258,165	(Satheshkumar et al., 2014; MassBank. 2023)
23.	10.418	Apigenin	C ₁₅ H ₁₀ O ₅	[M-H] ⁻	269.0461	269.0450	4.0885	269,225,151,117	(Abdelhameed et al., 2021; Abbas et al., 2022)
24.	10.712	Diosmetin	C ₁₆ H ₁₂ O ₆	[M-H] ⁻	299.0561	299.0556	1.6719	299	(Elmongy et al., 2022)
25.	10.771	Naringenin	C ₁₅ H ₁₂ O ₅	[M-H] ⁻	271.06119	271.0606	2.1766	271,151	(Elmongy et al., 2022; Chen et al., 2020)
26.	12.609	Hesperetin	C ₁₆ H ₁₄ O ₆	[M + H] ⁺	301.0876	303.0869	4.9822	153, 303	(Tong et al., 2012; MassBank. 2023)
27.	15.810	Acacetin	C ₁₆ H ₁₂ O ₅	[M-H] ⁻	283.0605	283.0606	-0.3533	268, 283	(Chen et al., 2020)
Anthocyanins									
28.	4.213	Cyanidin-3-O-glucoside	C ₂₁ H ₂₁ O ₁₁	[M-2H] ⁻	447.0944	447.0922	4.9207	447,284	(Elhady et al., 2022; MassBank. 2023)
29.	5.620	Delphinidin 3-O-rutinoside	C ₂₇ H ₃₁ O ₁₆	[M-2H] ⁻	609.1458	609.1450	1.3133	609	(Hegazy et al., 2022)
30.	7.804	Petunidin-3-O-β-glucopyranoside	C ₂₂ H ₂₃ O ₁₂	[M] ⁺	479.1224	479.1184	8.3487	479,317,302,285	(Abdel Maboud, 2021; Negm et al., 2022a)
Chalcones									
31.	3.681	Okanin-4'-O-glucoside	C ₂₁ H ₂₂ O ₁₁	[M-H] ⁻	449.1064	449.1084	-4.4533	449, 431	(Abbas et al., 2022)
32.	7.630	Phlorizin	C ₂₁ H ₂₄ O ₁₀	[M-H] ⁻	435.1293	435.1291	0.4596	435,433,389,273,167	(El-Hawary et al., 2021; Negm et al., 2022a)

(continued on next page)

Table 3 (continued)

Compound No.	Rt (min)	Proposed compound	Molecular formula	Precursor type	Obs. m/z for Precursor	Calcd. m/z for Precursor	Mass error	MS/MS	Ref.
33.	8.295	4-deoxy phloridzin	C ₂₁ H ₂₄ O ₉	[M-H] ⁻	419.1357	419.1342	3.5788	419,257	(Tsugawa et al., 2019; Abdelhameed et al., 2021)
Anthraquinones									
34.	2.152	Sennoside A	C ₄₂ H ₃₈ O ₂₀	[M-H] ⁻	861.1897	861.1897	0.0000	341,681,699, 861	(Ye et al., 2007; Zibae et al., 2023)
35.	7.781	Rhein	C ₁₅ H ₈ O ₆	[M-H] ⁻	283.0245	283.0243	0.70	239,257, 283	(Ye et al., 2007; Fu et al., 2015)
36.	13.612	Emodin	C ₁₅ H ₁₀ O ₅	[M-H] ⁻	269.0450	269.0450	-	225,241, 269	(MassBank, 2023,81,83,84)
37.	18.951	Chrysophanol	C ₁₅ H ₁₀ O ₄	[M-H] ⁻	253.0515	253.0501	5.5325	225,253	(Ye et al., 2007; Fu et al., 2015)
Coumarins									
38.	4.227	Daphnetin	C ₉ H ₆ O ₄	[M-H] ⁻	177.0198	177.0188	5.6491	177,133	(Tong et al., 2012; Abbas et al., 2022)
39.	4.278	Esculin	C ₁₅ H ₁₆ O ₉	[M-H] ⁻	339.0735	339.0716	5.6035	339,177	(Elhady et al., 2022)
40.	7.283	Scopoletin	C ₁₀ H ₈ O ₄	[M + H] ⁺	193.0514	193.0501	6.7340	193,133	(Abbas et al., 2022)
Phenolic acids and their derivatives									
41.	1.312	Gentisic acid	C ₇ H ₆ O ₄	[M-H] ⁻	153.0187	153.0188	-0.6535	153,108	(Wang et al., 2013; Abdelhameed et al., 2021)
42.	1.874	<i>p</i> -Coumaric acid	C ₉ H ₈ O ₃	[M-H] ⁻	163.0387	163.0395	-4.9068	163,119	(Chou et al., 2021)
43.	2.086	Ferulic acid	C ₁₀ H ₁₀ O ₄	[M-H] ⁻	193.0510	193.0501	4.6620	193,178,134	(Zhelong et al., 2020; Abdelhameed et al., 2021)
44.	2.205	Sinapic acid	C ₁₁ H ₁₂ O ₅	[M-H] ⁻	223.0608	223.0606	0.8966	223,208,149	(Abbas et al., 2022)
45.	3.228	<i>p</i> -Salicylic acid	C ₇ H ₆ O ₃	[M-H] ⁻	137.0247	137.0239	5.8384	137,93	(Abbas et al., 2022)
46.	6.424	5-Methoxysalicylic acid	C ₈ H ₈ O ₄	[M-H] ⁻	167.0354	167.0344	5.9868	167,152	(Elmongy et al., 2022)
47.	9.941	Syringaldehyde	C ₉ H ₁₀ O ₄	[M-H] ⁻	181.0494	181.0501	-3.8663	181	(Paganelli et al., 2020)
Stilbenoids									
48.	5.807	Astringin	C ₂₀ H ₂₂ O ₉	[M-H] ⁻	405.1196	405.1186	2.4684	405,243	(Elmongy et al., 2022; Attallah et al., 2021)
49.	9.109	Resveratrol	C ₁₄ H ₁₂ O ₃	[M-H] ⁻	227.0728	227.0708	8.8078	227, 185	(Sun et al., 2007)
Miscellaneous									
50.	5.449	Vitamin B2	C ₁₇ H ₂₀ N ₄ O ₆	[M + H] ⁺	377.1434	377.1461	-7.1590	377,243,198,172	(Abbas et al., 2022)
51.	3.004	Mandelic acid	C ₈ H ₈ O ₃	[M-H] ⁻	151.0403	151.0395	5.2966	151,125	(Zhong et al., 2020)
52.	1.209	Quinic acid	C ₇ H ₁₂ O ₆	[M-H] ⁻	191.0567	191.0556	5.7575	191,173,111,85	(Karar and Kuhnert 2015; Fan et al., 2017)
53.	1.338	Tagatose	C ₆ H ₁₂ O ₆	[M-H] ⁻	179.057	179.0556	7.8188	179,89	(Abbas et al., 2022)
54.	14.982	Glycyrrhizate	C ₄₂ H ₆₂ O ₁₆	[M-H] ⁻	821.3917	821.3960	-5.2350	821,775	(Elmongy et al., 2022)
55.	20.040	γ -Linolenic acid	C ₁₈ H ₃₀ O ₂	[M-H] ⁻	277.2176	277.2168	2.8858	277,259,233,59	(Abbas et al., 2022)

UCSF and AutoDock Vina on Linux-based systems. Binding sites within proteins were identified by measuring the sizes of grid boxes covering the co-crystallized ligands after their structures had been generated and optimized in Maestro. Following standard procedures (Nafie et al., 2019; Kishk et al., 2020; Kishk et al., 2022), the studied compounds were docked against the Caspase 3 (PDB = 6 CKZ) and COX-2 (PDB = 5 W58) protein structures using AutoDock Vina software. The results of molecular docking, interpreting binding activities in terms of binding energy and ligand-receptor interactions, were analyzed.

2.8. Statistical analysis

SPSS version 20 was employed to conduct the statistical analysis. The data were presented as means \pm S.E. via Duncan's new multiple range test (MRT) and One-Way Analysis of Variance (ANOVA). P values \leq 0.05 were considered statistically significant.

3. Results and Discussion

3.1. Total phenolic content (TPC) and flavonoid content(TFC)

As displayed in Table 1, the solvents used for extraction and fractionation influenced the estimated TPC and TFC. Among the tested samples, the EtOAc fraction of *C. fistula* showed the highest TPC (12.36

\pm 1.46 mg GAE/g) and TFC (5.12 \pm 0.64 mg. QE/100 mg) followed by n. butanol fraction of *C. fistula* with TFC of 5.03 \pm 0.94 mg QE/100 mg) and TPC of 11.47 \pm 1.29 mg GAE/ 100 mg then the crude extract with TFC and TPC of 4.25 \pm 0.71 mg QE/ 100 mg and 10.56 \pm 1.32 mg GAE/ 100 mg, respectively. The CHCl₃ exhibited notable TPC and TFC while n. hexane fraction recorded the least TFC and TPC.

High flavonoid and phenolic contents in medicinal plants are linked to antioxidant activity, which plays a vital role in the prevention and treatment of several chronic conditions caused by oxidative stress (Keshavarzi et al., 2019). The hexane fraction had the lowest TPC and TFC amounts of the crude extract and fractions, whereas the ethyl acetate (EtOAc) fraction had the greatest contents of total phenolic and flavonoids. These results agreed with earlier investigations that compared the influence of different solvents on the derivation of plant polyphenols and indicated that EtOAc is selectively the best solvent for extracting phenolic compounds, especially flavonoids (Das et al., 2014; Pintac et al., 2018; Autor et al., 2022).

3.2. Antioxidant Activity of crude extract and its EtOAc fraction

Three distinct antioxidant tests (TAC, FRAP, and DPPH) were used to assess the *in vitro* antioxidant activity of crude extract and EtOAc fraction. In Table 2, both the EtOAc fraction and the crude extract exhibited notable TAC with 65.19 \pm 5.33 mg GAE/g and 48.37 \pm 3.19 mg GAE/g

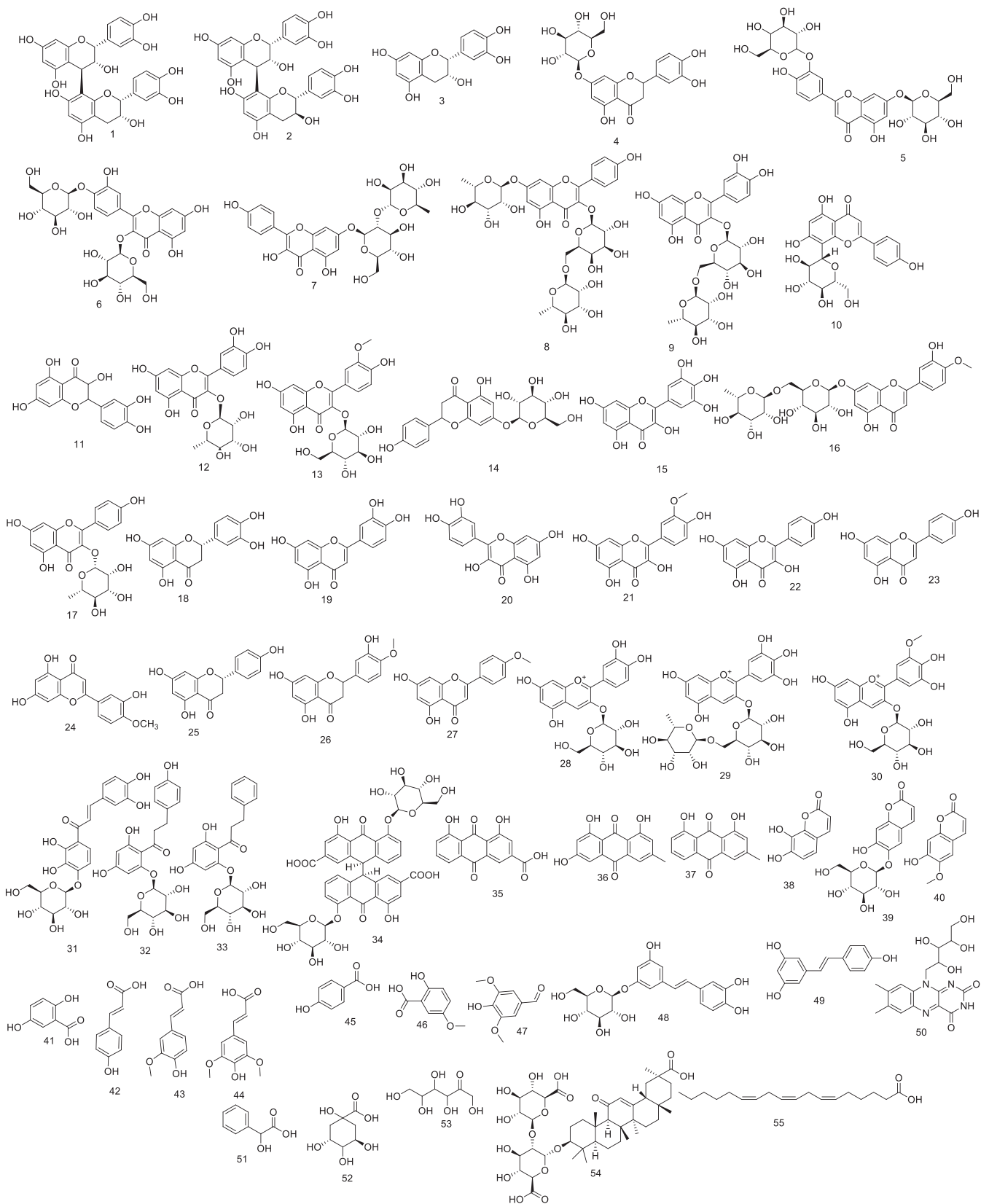


Fig. 3. Chemical structures identified by LC-MS/MS.

Table 4Protection and treatment effects of *C. fistula* on rat body weight and colon weight-to-length ratio in AA-induced colitis.

Groups	% change in body weight	Colon weight (g)	weight/length ratio (g/cm)	Microscopic scores
I	19.45 ± 1.29	2.42 ± 0.063	0.13 ± 0.003	normal stool consistency (0)
II	-15.89 ± 2.65 ^a	3.91 ± 0.14	0.21 ± 0.01 ^a	Water diarrhea (4)
III	31.16 ± 1.71 ^b	3.46 ± 0.32	0.18 ± 0.02 ^b	Loose stool (2)
IV	35.29 ± 2.00 ^b	2.89 ± 0.14	0.15 ± 0.01 ^b	Loose stools (3)
V	44.05 ± 2.58 ^b	2.85 ± 0.16	0.15 ± 0.01 ^b	(1)
VI	35.08 ± 2.53 ^b	2.67 ± 0.09	0.14 ± 0.00 ^b	(2)
VII	36.30 ± 0.60 ^{b,e}	3.10 ± 0.12	0.16 ± 0.01 ^{b,d}	(1)

respectively compared to that of BHT (the positive control; 76.43 ± 3.89 mg GAE/g).

In comparison to the positive control (BHT with 6.98 mMol Fe⁺²/g), the FRAP results showed that crude extract and its EtOAc fraction demonstrated promising ferric reduction ability with 2.76 and 4.87 mMol Fe⁺²/g, respectively (Table 2). The process involves observing a shift in absorbance, where a higher absorbance indicates increased reduction capacity in the tested samples. This method allows measurement and assessment of the compounds' ability to undergo reduction reactions (Nishikimi et al., 1972).

The crude extract as well as its EtOAc fraction had definite and remarkable quenching activity on DPPH free radical exhibiting a dose-dependent scavenging rate (Figs. 1 and 2). The calculated IC₅₀ of EtOAc fraction was 12.7 ± 0.94 µg/mL while that of the crude extract was 60.6 ± 3.46 µg/mL compared to the positive control (Ascorbic acid IC₅₀ = 10.6 ± 0.8 µg/mL) (Table 2).

3.3. Metabolite profiling of *C. fistula* leaf methanol extract

The Phyto-metabolomics of *C. fistula* was scrutinized by the hyphenated analysis; LC-ESI-TOF-MS/MS (Figures S1- S4). *C. fistula* metabolites were tentatively recognized by comparing the *m/z* values of the precursor ions, MS² fragmentation pattern, and retention times compared to those documented in the literature and mass spectrum data. Herein, 55 natural products were determined in extract, of which 50 compounds were phenolics. The dominant phenolic class was flavonoids (Table 3, Fig. 3).

This passage highlights the identification of various flavan-3-ols, flavones, flavonols, and flavanones in *C. fistula*. While epicatechin and

procyanidin B2 were previously reported in *C. fistula*, procyanidin A2 and epiafzelechin were newly discovered, differing from the previously recorded procyanidin B1 (Tan et al., 2018; Kaur et al., 2020; Aabideen et al., 2021; Sharma et al., 2021; Kanwal et al., 2022; Omer et al., 2022). Eriodictyol-7-O-glucoside, kaempferol-3-O-robinoside-7-O-rhamnoside, vitexin, taxifolin, hesperetin, naringenin-7-O-glucoside, quercetin-3,4'-O-di-β-glucopyranoside, and diosmin were found in the Cassia genus for the first time. Additionally, kaempferol-3-O-rhamnoside (Costa Silva et al., 2019) and diosmetin (Alhawarri et al., 2023) were recognized for the first time in this specific plant species. Notably, eriodictyol-7-O-neohesperidoside (Thabit et al., 2018; Kanwal et al., 2022), previously identified in *C. fistula*, was not detected; instead, its aglycone was present.

Three anthocyanins were recognized; Cyanidin-3-O-glucoside and petunidin-3-O-β-glucopyranoside were recorded in *C. fistula* before (Omer et al., 2022) while delphinidin 3-O-rutinoside was identified in the plant for the first time. Three chalcones were observed of which phlorizin was reported previously in *C. fistula* (Omer et al., 2022) however the others; okanin-4'-O-glucoside and 4-deoxy phloridzin have not been reported before in the plant.

All the detected anthraquinones in the present study (rhein, emodin, chrysophanol, and sennoside A) were identified before in the plant. However, other anthraquinones such as sennoside B, physcion, chrysophanol 1-O-glucoside (chrysophanein) 1-O-methyl chrysophanol, and the glucosides of both emodin and rhein reported earlier in *C. fistula* were not found (Sharma, 2021; Aabideen et al., 2021; Sharma et al., 2021; Kanwal et al., 2022).

Esculin, daphnetin, and scopoletin are coumarin compounds recorded in our extract among which scopoletin was detected before in



Fig. 4. Macroscopic imaging: A) Shows the colonic section of the control group (Group I), B) The colonic section of acetic-acid-induced colitis (Group II). C) The colonic section of the sulfasalazine-treated group (Group III). D) The colonic section of the pretreated group with a low dose (Group IV). E) The colonic section of the pretreated group with a high dose (Group V). F) The colonic section of the treated group with a low dose (Group VI). G) The colonic section of the treated group with a high dose (Group VII).

Table 5
Protection and treatment effects of *C. fistula* on red blood cells and their indices.

Groups	RBCs	HGB	HCT	MCV	MCH	MCHC	PLT
I	6.83 ± 0.18	13.85 ± 0.12	42.5 ± 0.41	94.5 ± 4.49	30 ± 1.63	32.5 ± 0.41	524.5 ± 26.54
II	5.33 ± 0.10 ^a	11.6 ± 0.40 ^a	36 ± 1.32 ^a	61.33 ± 0.76 ^a	19.33 ± 0.58 ^a	31.67 ± 0.29	902.33 ± 26.57 ^a
III	7.87 ± 0.38 ^b	14.87 ± 0.35 ^b	46.13 ± 1.91 ^b	58.63 ± 1.48	18.93 ± 0.62	32.3 ± 0.58	709.67 ± 12.20 ^b
IV	7.77 ± 0.18 ^b	16.83 ± 0.62 ^b	43.40 ± 1.75 ^b	57.8 ± 1.21	22.27 ± 0.52 ^{b,e}	38.43 ± 1.52 ^{b,e}	691.67 ± 42.18 ^b
V	7.23 ± 0.32 ^b	14.73 ± 0.24 ^{b,c}	43.63 ± 1.71 ^b	59.9 ± 0.68	20.3 ± 0.68	33.83 ± 0.87	612 ± 36.69 ^b
VI	6.67 ± 0.18 ^{b,e}	12.93 ± 0.55 ^b	39.37 ± 1.16 ^b	57.93 ± 0.95	19.03 ± 0.52	32.87 ± 1.21	674 ± 36.69 ^b
VII	7.2 ± 0.35 ^b	12.17 ± 1.35	45 ± 0.58 ^{b,d}	63.47 ± 2.59	19.47 ± 1.3	32.57 ± 1.87	819.33 ± 61.33

Data presented as mean ± S.E (n = 5). RBCs; red blood cells, HGB; hemoglobin, HCT; hematocrit, MCV; mean corpuscular volume, MCH; mean corpuscular hemoglobin, MCHC; mean corpuscular hemoglobin concentration, and PLT; platelet. I; control, II; acetic acid, III; treated with sulfasalazine drug, IV; protection with a low dose (200 mg/kg), V; protection with a high dose (400 mg/kg), VI; treatment with a low dose and VII; treatment with a high dose. ^a significant difference as compared to control, ^b Significant difference as compared to acetic acid, ^c significant difference as compared to protection with a low dose, ^d significant difference as compared to treatment with a low dose of leaf crude extract, and ^e significant difference as compared to treatment with sulfasalazine drug ($p \leq 0.05$).

Table 6
Protection and treatment effects of *C. fistula* on blood differential leukocyte of rats.

Groups	WBCs	Band/Staff	Neutrophils	Lymphocytes	Monocytes	Eosinophils	Basophils
I	6.35 ± 0.12	1.5 ± 0.41	61.5 ± 2.04	30.5 ± 2.04	5.50 ± 0.41	3.50 ± 0.41	–
II	18.85 ± 1.67 ^a	2.33 ± 0.29	60.33 ± 2.93	30.33 ± 1.53	6.33 ± 0.76	2.00 ± 0.00 ^a	–
III	13.7 ± 0.86	1.33 ± 0.33	5.67 ± 0.33 ^b	75.33 ± 0.88 ^b	3.33 ± 0.33 ^b	14.67 ± 1.20 ^b	–
IV	11.3 ± 1.66 ^b	1.67 ± 0.33	9.67 ± 1.76 ^b	35.33 ± 2.67 ^e	4.67 ± 0.67	3.33 ± 0.33 ^{b,e}	–
V	14.3 ± 1.46	2.00 ± 0.58	14.00 ± 2.08 ^{b,e}	77.33 ± 2.19 ^{b,c}	5.67 ± 1.20	5.33 ± 1.45 ^e	–
VI	15.4 ± 1.91	0.33 ± 0.33 ^b	5.00 ± 0.58 ^b	75.67 ± 0.88 ^b	3.33 ± 0.33 ^b	16.33 ± 1.45 ^b	–
VII	20.7 ± 1.75 ^e	0.67 ± 0.33 ^b	5.00 ± 0.58 ^b	73.67 ± 1.76 ^b	4.67 ± 0.33 ^{d,e}	17.67 ± 1.45 ^b	–

C. fistula (Sharma, 2021; Kanwal et al., 2022). However, esculin and daphnetin were detected for the first time. Nevertheless, several reported coumarins such as isoscoupoletin, esculetin, 2,5-dimethyl-7 hydroxy chromone, and umbelliferone identified earlier in the plant (Kanwal et al., 2022;48] were not recognized.

Our extract is rich in phenolic acids and their derivatives. Among the detected phenolic acids, *p*-coumaric, ferulic (Kanwal et al., 2022; Omer et al., 2022), and sinapic acid (Kaur et al., 2020) were reported before in the plant (Tan et al., 2018; Kanwal et al., 2022). While gentisic, *p*-salicylic, and 5-Methoxysalicylic acids were recognized for the first time in *C. fistula*. An earlier study has reported the presence of syringic acid in the plant (Omer et al., 2022) however, it was not identified in the current study. Instead, we pick up its aldehyde derivative (syringaldehyde). On the other hand, other reported phenolic acids (Laxmi et al., 2015; Kanwal et al., 2022; Omer et al., 2022) such as gallic, ellagic, vanillic chlorogenic, and caffeic cinnamic acids were not recorded.

Astringin and resveratrol are naturally occurring stilbenes. Astringin was determined in the genus *Cassia* (family: Fabaceae). Meanwhile, resveratrol was found in *C. fistula* (Kusumaningtyas et al., 2020).

Besides the detected phenolics, other non-phenolic compounds were observed belonging to various phytochemical classes including vitamins (riboflavin), organic acids (mandelic and quinic acids), sugars (tagatose), fatty acids (γ -linolenic acid) and triterpenes (glycyrrhizate). All these compounds are identified for the first time in *C. fistula* except

Table 7
Protection and treatment effects of *C. fistula* on the liver functions of rats.

Groups	ALT (U/L)	AST (U/L)	Total Bilirubin (mg/dl)	ALP (U/L)	Total protein (g/dl)
I	29.5 ± 0.87	54.33 ± 2.85	0.62 ± 0.02	556 ± 3.06	9.1 ± 0.31
II	64 ± 3.61 ^a	135.67 ± 0.88 ^a	0.8 ± 0.06 ^a	2011.67 ± 65.90 ^a	6.03 ± 0.15 ^a
III	45 ± 0.58 ^b	100.6 ± 1.55 ^b	0.3 ± 0.06 ^b	199.63 ± 6.12 ^b	7.07 ± 0.55
IV	24.67 ± 2.96 ^{b,e}	82.33 ± 2.19 ^{b,e}	1.0 ± 0.06 ^e	200.33 ± 15.94 ^b	7.1 ± 0.26 ^b
V	30 ± 1.53 ^{b,e}	73.67 ± 2.19 ^{b,c,e}	0.97 ± 0.15 ^e	412.73 ± 3.82 ^{b,c,e}	9.3 ± 0.6 ^{b,c}
VI	51.33 ± 3.48	93.6 ± 5.98 ^b	0.37 ± 0.03 ^b	314.47 ± 18.01 ^{b,e}	5.8 ± 0.47
VII	51.43 ± 1.29 ^{b,e}	39.07 ± 2.76 ^{b,d,e}	0.37 ± 0.03 ^b	412.73 ± 11.11 ^{b,d,e}	7.77 ± 0.49 ^{b,d}

Data presented as mean ± S.E (n = 5). ALT; alanine aminotransferase, AST; aspartate aminotransferase, and ALP; Alkaline phosphatase I; control, II; acetic acid, III; treated with sulfasalazine drug, IV; protection with a low dose, V; protection with a high dose, VI; treatment with a low dose and VII; treatment with a high dose. ^a significant difference as compared to control, ^b Significant difference as compared to acetic acid, ^c significant difference as compared to protection with a low dose, ^d significant difference as compared to treatment with a low dose, and ^e significant difference as compared to treatment with sulfasalazine drug ($p \leq 0.05$).

γ -linolenic acid (Kanwal et al., 2022). These findings highlight that the antioxidant activity exhibited by the extract is attributed to phenolics rather than other compounds since the former chemical class preponderates in *C. fistula*. Therefore, this justifies why the EtOAc displayed higher antioxidant activity compared to crude extract.

3.4. In vivo study

3.4.1. Rat body weight and colon weight-To-length ratio in AA-induced colitis

Acetic acid (AA) led to a notable decrease in rat body weight within the positive control group. Simultaneously, in the UC (ulcerative colitis) group, AA significantly increased the ratio of wet weight to length, a marker comparable to that of the negative control rats. When compared to the UC group, treatment with sulfasalazine demonstrated a significant decrease in the wet weight/length ratio and showed a notable increase in the percentage change in rat body weight, particularly when administered alongside prevention and treatment involving *C. fistula* at doses of 200 mg/kg/day and 400 mg/kg (Table 4). The disease activity index of cores of colitis is mentioned in Table 4.

Data presented as mean ± S.E (n = 5). Colon length = 19 cm. I; control, II; acetic acid, III; treated with sulfasalazine drug, IV; protection with a low dose (200 mg/kg), V; protection with a high dose (400 mg/kg), VI; treatment with a low dose and VII; treatment with a high dose. ^a

Table 8Protection and treatment effects of *C. fistula* on the oxidative/antioxidant parameters of colon rats.

Groups	MDA	SOD	CAT	GPx	GSH	TAC
I	503.33 ± 1.76	941.67 ± 4.17	13.87 ± 0.49	18.48 ± 0.72	42.33 ± 3.33	0.64 ± 0.03
II	857 ± 11.53 ^a	870.17 ± 17.63 ^a	4.87 ± 0.05 ^a	52.42 ± 2.97 ^a	12.33 ± 0.88 ^a	0.43 ± 0.03 ^a
III	870 ± 3.51	3249.99 ± 1.16 ^b	14.03 ± 1.16 ^b	18.74 ± 0.43 ^b	37.00 ± 1.15 ^b	0.47 ± 0.03
IV	955.67 ± 24.18 ^{b,e}	924.33 ± 7.25 ^{b,e}	14.82 ± 1.38 ^b	131.78 ± 4.39 ^{b,e}	16.67 ± 1.2 ^{b,e}	0.37 ± 0.09
V	577.67 ± 8.09 ^{b,c,e}	941.67 ± 4.17 ^{b,e}	12.15 ± 0.47 ^b	94.81 ± 2.45 ^{b,c,e}	16.33 ± 1.76 ^e	0.17 ± 0.03 ^{b,e}
VI	1015 ± 1.73 ^{b,e}	1895.83 ± 41.67 ^{b,e}	15.86 ± 1.08 ^b	18.91 ± 0.31 ^b	16.33 ± 0.33 ^{b,e}	0.47 ± 0.03
VII	562.67 ± 11.89 ^{b,d,e}	3770.83 ± 3.19 ^{b,d,e}	8.77 ± 0.41 ^{b,d,e}	55.29 ± 3.19 ^{d,e}	27.00 ± 0.58 ^{b,d,e}	0.33 ± 0.07

Data presented as mean ± S.E (n = 5). MDA; malondialdehyde, SOD; superoxide dismutase, CAT; catalase, GPx; glutathione peroxidase, GSH; reduced glutathione, TAC; total antioxidant capacity. I; control, II; acetic acid, III; treated with sulfasalazine drug, IV; protection with a low dose, V; protection with a high dose, VI; treatment with a low dose and VII; treatment with a high dose. ^a significant difference as compared to control, ^b Significant difference as compared to acetic acid, ^c significant difference as compared to protection with a low dose, ^d significant difference as compared to treatment with a low dose, and ^e significant difference as compared to treatment with sulfasalazine drug ($p \leq 0.05$).

significant difference as compared to control, ^b Significant difference as compared to acetic acid, ^c significant difference as compared to protection with a low dose, ^d significant difference as compared to treatment with a low dose, and ^e significant difference as compared to treatment with sulfasalazine drug ($p \leq 0.05$). Macroscopic inflammation scores were assigned based on clinical features of the colon using an arbitrary scale ranging from 0 to 4 as follows: 0 (no macroscopic changes), 1 (mucosal erythema only), 2 (mild mucosal edema, slight bleeding or small erosions), 3 (moderate edema, slight bleeding ulcers or erosions), 4 (severe ulceration, edema, and tissue necrosis)

The phenolic bioactive chemicals, which are present in variable amounts in different extracts of *C. fistula* can operate either individually or synergistically to give rise to their antioxidant capabilities and pharmacological effects. Motivated by the aforementioned considerations, we have evaluated the therapeutic potential (as a prophylaxis and treatment) of *C. fistula* against acetic acid-induced UC in rats. In the current study, AA was administered intra-rectally causing a drastic reduction in the body weight of the rats. Weight loss in colitis is brought on by dietary deficiencies due to decreased appetite, food aversion or malabsorption, and rapid loss of bodily fluids owing to diarrhea and colon hemorrhage. These observations are in parallel with a study described by Owusu et al. (2020). The body weight is significantly affected by the standard drug and extract. The protection with the extract is more effective in the body weight than the treatment,

especially when using a high dose.

3.4.2. Macroscopic alterations in AA-induced UC

After being longitudinally opened and sanitized with ordinary saline, colons were examined (Fig. 4A-4G). When the colons of the control group were inspected, it was found that the mucosa and serosa were both intact and there were no signs of tissue loss or bleeding (Fig. 4A). Investigation revealed considerable bleeding, extensive ulceration, and tissue edema over a sizable surface area in the acetic acid-induced group (Fig. 4B). Erosions and damage to the mucosal lining were seen (green arrows). Sulfasalazine and treated groups showed the best level of protection against mucosal injury and tissue necrosis, both at high and low dosages, with no obvious bleeding (Fig. 4C, 4E, and 4G). Pretreated groups did not have severe damage to the rat colons or tissue erosions, despite the slight bleeding (Fig. 4D).

A considerable rise in the rats' colon weight/length ratio was seen in the AA group. This is due to goblet cell hyperplasia, necrosis, severe tissue edema, and inflammatory cell infiltration (El-Abhar et al., 2008). When rats were treated with methanol-leaf extract (MLE), fecal pellets free of obvious blood or mucus stains were observed. This could be a result of the mucus layer not being damaged and the prevention of severe blood loss, both of which are indications that prospective anti-ulcerative medications were successful in preventing the condition (Al-Rejaie et al., 2012; Owusu et al., 2020). It is well known that the

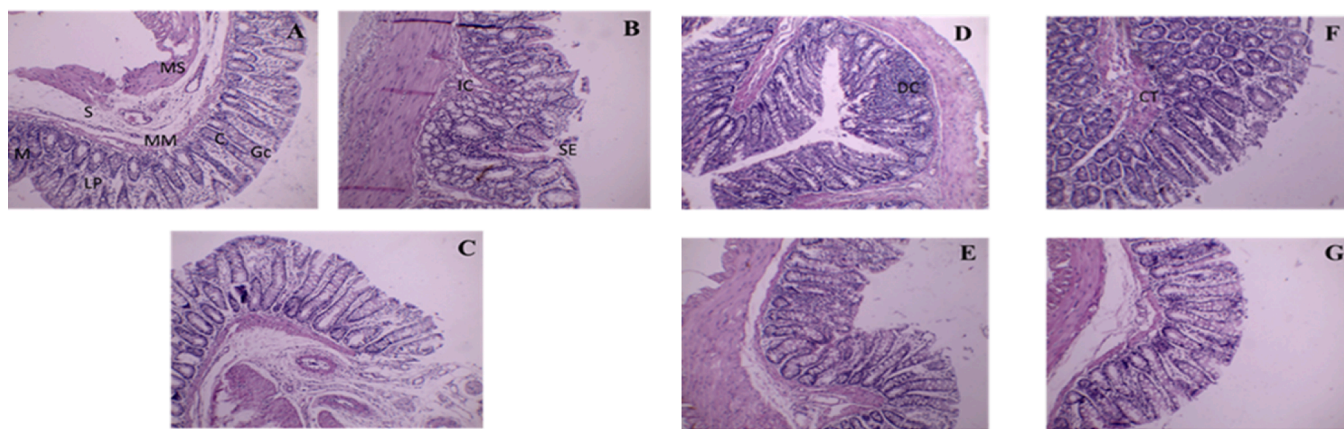


Fig. 5. (A-G) Light micrographs of colonic mucosa. A) Control rats showing, normal architecture, and arrangement of the lining layers; mucosa (M), muscularis mucosa (MM), submucosa (S), and musculus (MS). Apical parts of the mucosa; absorptive crypt cells I, numerous Goblet cells (GC), and obvious lamina propria (LPB). B) colonic mucosa was observed 17 days after induction of colitis and oral treatment with saline, with some generation in the acetic acid group. Showing, IC: invasion of some inflammatory cells, separation of the epithelium (SE), and damaging crypts (DC). C) Colonic mucosa 17 days after induction of colitis and oral treatment with sulfasalazine. Showing, maintained the regular arrangement of cell structure, epithelium remained intact and Goblet cells and crypts were both normally distributed. D) Colonic mucosa observed 17 days after pretreatment with a low dose extract to induce colitis; showing alteration in mucosal, submucosal, and musculosal layers, with damaged crypts. E) colonic mucosa observed 17 days after pretreatment with a high dose to induced colitis: minimal inflammatory reaction in the mucosa and submucosa without any feature of tissue destruction. Note also, that Crypts had a normal architecture with intact vacuolated goblet cells. F) colonic mucosa observed 17 days after induction of colitis and oral treatment with a low dose; more connective tissue cells (CT) and increased number of crypts. G) Colonic mucosa 17 days after induction of colitis and oral treatment with a high dose; the treatment ameliorates.

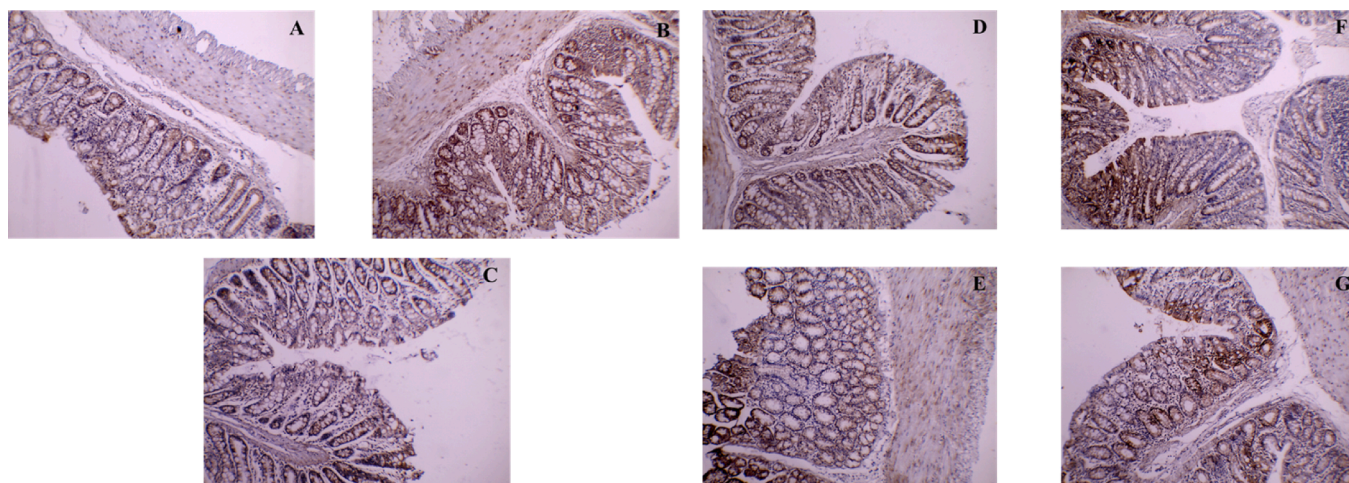


Fig. 6. COX-2 immunostaining. A) Shows control COX-2 expression (Group I), brown color indicates specific immunostaining of cleaved COX-2 and light blue color indicates nuclear hematoxylin staining. B) The colonic section of acetic-acid-induced colitis (Group II) depicts numerous cells with a strong positive mainly cytoplasmic COX-2 reaction. C) The colonic section of the sulfasalazine-treated group (Group III) shows a near-control COX-2 expression. D) The colonic section of the pretreated group with a low dose (Group IV); shows multiple cells with a moderately positive cytoplasmic COX-2. E) The colonic section of the pretreated group with a high dose (Group V); reaction reveals few cells with a weak positive cytoplasmic COX-2 reaction. F) The colonic section of the treated group with a low dose (Group VI); shows multiple cells with a moderately positive cytoplasmic COX-2. G) The colonic section of the treated group with a high dose (Group VII); shows a near-control COX-2 expression. [Original magnification: 40x].

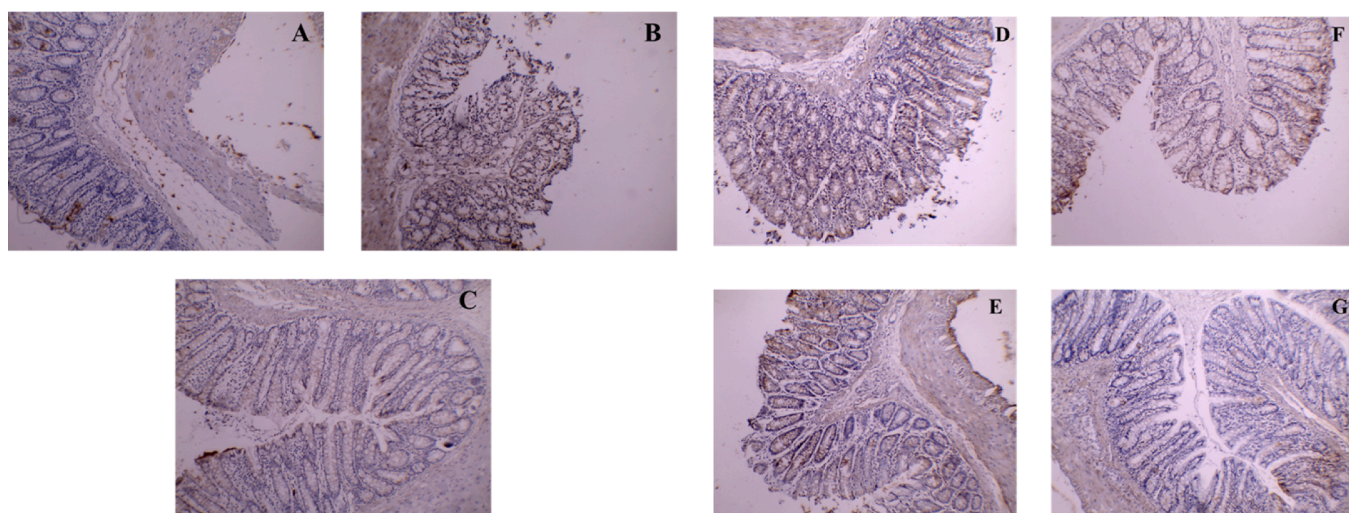


Fig. 7. Caspase-3 immunostaining. A) Shows control caspase-3 expression (Group I), brown color indicates specific immunostaining of cleaved caspase-3 and light blue color indicates nuclear hematoxylin staining. B) The colonic section of acetic-acid-induced colitis (Group II) depicts numerous cells with a strong positive mainly nuclear caspase-3 reaction. C) The colonic section of the sulfasalazine-treated group (Group III) shows a near-control caspase-3 expression. D) The colonic section of the pretreated group with a low dose (Group IV); shows multiple cells with a moderately positive cytoplasmic caspase-3. E) The colonic section of the pretreated group with a high dose (Group V); reaction reveals few cells with a weak positive cytoplasmic caspase-3 reaction. F) The colonic section of the treated group with a low dose (Group VI); shows multiple cells with a moderately positive cytoplasmic caspase-3. G) The colonic section of the treated group with a high dose (Group VII); shows a near-control caspase-3 expression. [Original magnification: 40x].

mucus layer helps to speed up the healing of chemically caused epithelium injury and also reduces diarrhea and blood loss through feces (Awaad et al., 2017). Therefore, it should come as no surprise that MLE preservation of the mucus layer improved colonic ulceration. Our findings validate that administering MLE to rats before and after AA administration has a significant impact on UC. This is evident through the reduction in the macroscopic examination score, preservation of the intestinal mucosa, and a conspicuous decrease in inflammation of the colon tissue.

3.4.3. Hematological parameters and leukocytes

After acetic acid-induced colitis, the levels of RBCs, HGB, HCT, MCV, and MCH dramatically decreased as compared to the control group,

However, the level of PLT significantly increased (Table 5). Sulfasalazine-treated rats had significantly reduced PLT counts and significantly increased RBCs, HGB, and HCT levels when compared to positive control animals. Rats prophylactically administered low and high dosages of crude extract had considerably more RBCs, HGB, HCT, and PLT than UC animals. RBC and HCT levels considerably rose in the low and high treatment groups in comparison to the UC group. The number of RBCs in the low-dosage treatment and MCH and MCHC in the low-dose preventative groups both increased significantly as compared to the sulfasalazine-treated group.

In AA-induced colitis, the WBC count significantly increased while the eosinophil level significantly dropped in comparison to the control group (Table 6). Both the sulfasalazine-treated group and the ones

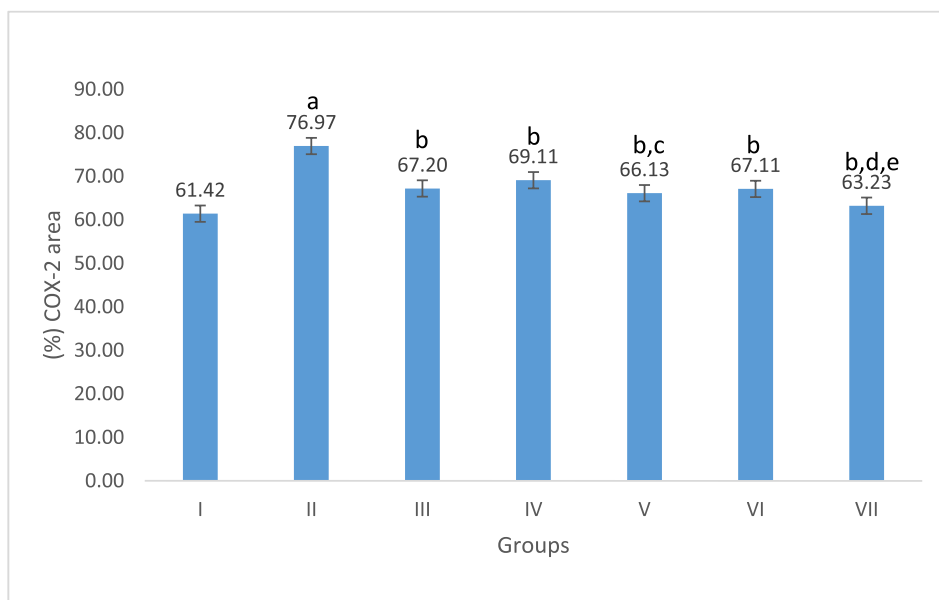


Fig. 8. Effect of *C. fistula* on COX-2 positively stained area percentage in colon rats. Data presented as mean \pm S.E (n = 5). I; control, II; acetic acid, III; treated with sulfasalazine drug, IV; protection with a low dose, V; protection with a high dose, VI; treatment with a low dose and VII; treatment with a high dose. ^a significant difference as compared to control, ^b Significant difference as compared to acetic acid, ^c significant difference as compared to protection with a low dose, ^d significant difference as compared to treatment with a low dose, and ^e significant difference as compared to treatment with sulfasalazine drug ($p \leq 0.05$).

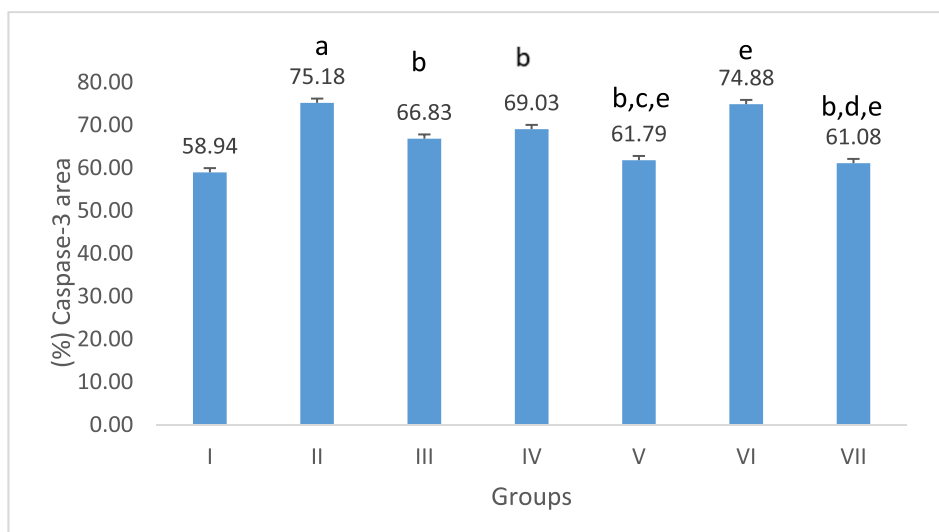


Fig. 9. Effect of *C. fistula* on caspase-3 positively stained area percentage in colon rats. Data presented as mean \pm S.E (n = 5). I; control, II; acetic acid, III; treated with sulfasalazine drug, IV; protection with a low dose, V; protection with a high dose, VI; treatment with a low dose and VII; treatment with a high dose. ^a significant difference as compared to control, ^b Significant difference as compared to acetic acid, ^c significant difference as compared to protection with a low dose, ^d significant difference as compared to treatment with a low dose, and ^e significant difference as compared to treatment with sulfasalazine drug ($p \leq 0.05$).

treated with low and high dosages of extract showed a significant decrease in neutrophils and monocytes, and a significant rise in lymphocytes and eosinophils. The number of WBCs and neutrophils significantly dropped in a low dose (200 mg/kg) prophylactic group of *C. fistula*. The number of RBCs in the low-dosage treatment group and MCH and MCHC in the low-dose preventative group both significantly increased in contrast to the sulfasalazine-treated group.

The WBC count significantly increased in acetic acid-induced colitis (Table 6). In the sulfasalazine-treated group, as well as in the low and high doses of *C. fistula*-treated groups, neutrophils, and monocytes were dramatically decreased, whereas lymphocytes and eosinophils were significantly increased. When the extract was administered prophylactically at 200 mg/kg, the number of WBCs and neutrophils drastically

decreased.

Data presented as mean \pm S.E (n = 5). WBCs are white blood cells. I; control, II; acetic acid, III; treated with sulfasalazine drug, IV; protection with a low dose, V; protection with a high dose, VI; treatment with a low dose and VII; treatment with a high dose. ^a significant difference as compared to control, ^b Significant difference as compared to acetic acid, ^c significant difference as compared to protection with a low dose, ^d significant difference as compared to treatment with a low dose, and ^e significant difference as compared to treatment with sulfasalazine drug ($p \leq 0.05$).

In current results, different outcomes were found for MLE therapy or protection on the hematological parameters. Reduced RBC characteristics have been associated with anemia brought by the AA treatment as

Table 9

Binding energy (Kcal/mol) of the docked compounds towards caspase-3 and COX-2 proteins.

Compound	Binding energy (Kcal/mol)	
	Caspase-3 PDB = 6 CKZ	COX-2 PDB = 5 W58
Procyanidin B2	-16.25	-15.26
Procyanidin B1	-9.6	-
Epicatechin	-10.36	-13.2
Eriodictyol-7-O-glucoside	-11.2	-
Luteolin-3', 7-di-O-glucoside	-16.8	-18.6
Quercetin-3,4'-O-di-β-glucopyranoside	-9.5	-10.3
Kaempferol-7-neohesperidoside	-10.3	-9.8
Kaempferol-3-O-robinoside-7-O-rhamnoside	-12.3	-8.9
Rutin	-11.36	-9.8
Vitexin	-7.36	-10.36
Taxifolin	-8.59	-8.9
Quercitrin	-9.58	-8.5
Hesperetin	-16.8	-9.5
Isorhamnetin-3-O-glucoside	-6.8	-
Naringenin-7-O-glucoside	-9.68	-8.9
Myricetin	-5.8	-12.3
Quercetin	-11.2	-8.9
Diosmin	-8.68	-11.2
Kaempferol-3-O-α-rhamnoside	-6.58	-13.2
Eriodictyol	-8.5	-10.2
Luteolin	-8.6	-13.2
Isorhamnetin	-19.4	-11.2
Apigenin	-5.26	-10.2
Diosmetin	-9.2	-11.1
Naringenin	-11.2	-10.1
Kaempferol	-16.2	-8.5
Acacetin	-10.2	-10.2
Cyanidin-3-O-galactoside	-16.9	-15.8
Delphinidin 3-O-rutinoside	-	-9.8
Petunidin-3-O-β-glucopyranoside	-13.1	-9.2
Okanin-4'-O-glucoside	-16.2	-15.6
Phlorizin	-13.2	-11.0
4-deoxy phloridzin	-13.6	-8.9
Senoside A	-	-
Rhein	-	-11.2
Emodin	-	-13.2
Chrysophanol	-	-13.1
Esculin	-11.3	-5.6
Daphnetin	-10.3	-12.3
Scopoletin	-10.3	-12.1
Gentisic acid	-	-6.3
p-Coumaric acid	-11.1	-4.5
Ferulic acid	-13.6	-5.6
Sinapic acid	-8.6	-5.60
p-Salicylic acid	-	-
5-Methoxysalicylic acid	-	-
Syringaldehyde	-	-5.7
Astringin	-12.3	-6.48
Resveratrol	-9.68	-3.4
Vitamin B2	-9.8	-4.5
Mandelic acid	-	-
Quinic acid	-	-
Tagatose	-	-
Glycyrrhizate	-10.3	-
γ-Linolenic acid	-	-

previously described (Alia et al., 2019). The WBCs elevated in the AA group as compared to control animals. According to a report, an increase or reduction in granulocyte cells corresponds to an increase or decrease in inflammatory activity (Alia et al., 2019). Sulfasalazine did not cause any significant change in differential leukocyte parameters that were assessed, these results are in agreement with Owusu et al. (2020).

3.4.4. Effect of *C. fistula* on liver functions in AA-induced colitis

All liver functions in the acetic acid-induced group showed significant changes in which ALT, AST, total bilirubin, and ALP increased significantly while total protein decreased significantly as compared to control animals (Table 7). ALT, AST, total bilirubin, and ALP were

Table 10

The compounds discovered exhibit ligand-receptor interactions toward the caspase-3 (PDB = 6 CKZ) and COX (PDB = 5 W58) proteins.

	Caspase-3 PDB = 6 CKZ	COX-2 PDB = 5 W58
	Co-crystallized ligand	2H-bond with His 121 Lipophilic interactions Arg 207
Procyanidin B2	1HB with Arg 207 1HB with His 121 1 Arene-cation His 121	1 HB with Ile 12 1 HB with Asp 15 1 Arene-cation His 13
Procyanidin B1	1HB with Arg 207	1 Arene-cation His 13
Epicatechin	1HB with Arg 207 1HB with His 121 2HB with Arg 207	2H-bonds with Tyr 355 and Arg 120 1 Arene-cation His 13
Eriodictyol-7-O-glucoside		1 HB with Asp 15 1 Arene-cation His 13
Luteolin-3', 7-di-O-glucoside	1 Arene-cation His 121	1 HB with Asp 15 1 Arene-cation His 13
Quercetin-3,4'-di-β-glucopyranoside	1 Arene-cation His 121 1HB with Arg 207	1 HB with Ile 12 1 Arene-cation His 13
Kaempferol-7-neohesperidoside	1 Arene-cation His 121 1HB with His 121	1 HB with Ile 12 1 Arene-cation His 13
Kaempferol-3-O-robinoside-7-O-rhamnoside	1 Arene-cation His 121 1HB with His 121	1 HB with Asp 15 1 Arene-cation His 13
Rutin	1HB with His 121 1 Arene-cation His 121	1 HB with Ile 12 1 HB with Asp 15
Vitexin	1 HB with His 121 1 HB with Arg 207	2H-bonds with Tyr 355 and Tyr 385
Taxifolin	1HB with Arg 207 1HB with His 121	1H-bond with Tyr 355 and Tyr 385
Quercitrin	1HB with Arg 207 1HB with His 121	1 HB with Ile 12 1 HB with Asp 15
Hesperetin	1 HB with Arg 64 1 HB with Arg 207 1 Arene-cation Arg 207	1 HB with Ile 12 1 HB with Asp 15
Isorhamnetin-3-O-glucoside	1HB with Arg 207	1 Arene-cation His 13
Naringenin-7-O-glucoside	1HB with Arg 207 1HB with His 121	1 HB with Ile 12 1 HB with Asp 15
Myricetin	1HB with Arg 207	2H-bonds with Tyr 355
Quercetin	1HB with Arg 207 1HB with His 121	1 HB with Ile 12 1 HB with Asp 15
Diosmin	1 Arene-cation His 121 1HB with Arg 207	2 HB with Ile 12
Kaempferol-3-O-α-rhamnoside	1HB with Arg 207 1HB with His 121	1 HB with Ile 12 1 HB with Asp 15
Eriodictyol	1HB with Arg 207	2 HB with Asp 15
Luteolin	1HB with His 121	2H-bonds with Tyr 355 and Arg 120
Isorhamnetin	1 HB with His 121 1 HB with Arg 207 1 Arene-arene His 121	1 HB with Ile 12 1 HB with Asp 15
Apigenin	1 HB with His 121	2H-bonds with Tyr 355 and Arg 120
Diosmetin	1 HB with Arg 207	1 HB with Ile 12 1 HB with Asp 15
Naringenin	1 HB with His 121 1 Arene-arene His 121	2 HB with Ile 12
Kaempferol	1 HB with Arg 207 1 Arene-arene Arg 207	1 HB with Ile 12 1 HB with Asp 15
Acacetin	2 HB with Arg 207	2 HB with Asp 15
Cyanidin-3-O-galactoside	1 Arene-cation His 121 1HB with Arg 207	1 HB with Ile 12 1 Arene-cation His 13
Delphinidin 3-O-rutinoside	1 Arene-arene His 121	1 HB with Ile 12 1 Arene-cation His 13
Petunidin-3-O-β-glucopyranoside	1 HB with His 121 1 Arene-arene Arg 207	1 Arene-cation His 13 1 HB with Asp 15

(continued on next page)

Table 10 (continued)

	Caspase-3 PDB = 6 CKZ	COX-2 PDB = 5 W58
Okaniin-4'-O-glucoside	1 HB with His 121 1 Arene-arene His 121	1 Arene-cation His 13 1 HB with Ile 12 1 HB with Asp 15
Phlorizin	2 HB with Arg 207	1 Arene-cation His 13 1 HB with Ile 12
4-deoxy phloridzin	2 HB with His 121	1 Arene-cation His 13 1 HB with Asp 15
Senoside A	–	1 Arene-cation His 13
Rhein	–	2H-bonds with Tyr 355, Ser 530
Emodin	–	2 HB with Ile 12 1 HB with Asp 15
Chrysophanol	–	1 HB with Ile 12 1 HB with Asp 15
Esculin	1 HB with His 121 1 HB with Arg 207	1 Arene-cation His 13 1 HB with Ile 12
Daphnetin	1 HB with His 121	2 HB with Ile 12 1 HB with Asp 15
Scopoletin	1 HB with Arg 207	1 HB with Ile 12 1 HB with Asp 15
Gentisic acid	–	1 HB with Ile 12
<i>p</i> -Coumaric acid	1 HB with His 121	1 HB with Ile 12
Ferulic acid	1 Arene-arene His 121 1 HB with His 121	1 HB with Ile 12 1 HB with Tyr 355
Sinapic acid	1 HB with His 121	1 HB with Ile 12 1 HB with Arg 120
<i>p</i> -Salicylic acid	–	–
5-Methoxysalicylic acid	–	–
Syringaldehyde	–	1 HB with Arg 120
Astringin	1 HB with His 121 1 HB with His 121	1 HB with Ile 12 1 HB with Asp 15
Resveratrol	1 HB with His 121	1 HB with Arg 120
Vitamin B2	1 HB with His 121 1 HB with Arg 207	1H-bonds with Tyr 355
Mandelic acid	–	–
Quinic acid	–	–
Tagatose	–	–
Glycyrrhizate	1 HB with Arg 207	–
γ -Linolenic acid	–	–

markedly decreased in the sulfasalazine-treated group when compared to the UC group. ALT and AST activities significantly decreased in low and high-dose preventative groups and high-dose treatment animals compared to the sulfasalazine-treated and UC rats.

The ALP activity decreased significantly in all prevention and treatment groups as compared to the UC rats (Table 7). The total protein increased by 1.17-, 1.54-, and 1.28-fold in low and high prevention groups as well as the high treated group as compared to UC animals, respectively (Table 7).

The administration of MLE considerably reduced the rise of ALP in groups treated for colitis; this effect may have been caused by the extract's possible anti-inflammatory properties. The outcomes concur with those of other authors (Sarkar et al., 2015; Hasona and Hussien, 2017) who reported a notable increase in ALP activity in the serum of rats with AA-induced colitis.

3.4.5. Effect of *C. fistula* on antioxidant and oxidative stress in aa-induced colitis

Examination of all rats' colons revealed the presence of MDA, a marker for LPO. Comparing the UC (ulcerative colitis) group to the control group, a significant elevation in colon MDA levels was observed (Table 8). This is indicated by tissue damage (Vishwakarma et al., 2015). However, rats receiving a high dose for prevention or treatment exhibited a noteworthy decrease in colon MDA levels compared to the

UC group. Additionally, the UC group displayed significantly reduced activity of SOD and CAT compared to the negative control group. Conversely, the activity of GPx in UC rats was notably increased compared to the control animals. Furthermore, levels of GSH and TAC declined significantly in the UC group compared to the negative control rats.

Treatment and protection of rats with a high dose (400 mg/kg/day) produced a marked significant decrease in LPO concentration that reached the control value ($562.67 \pm 11.89 \mu\text{mol/g}$ and 577.67 ± 8.09 , respectively). Interestingly, the activity of SOD and CAT along with the content of GSH showed significant restoration in the groups treated with sulfasalazine, both in the pretreatment and treated groups, compared to the UC (ulcerative colitis) animals (Table 8).

The existence of enzymatic and non-enzymatic antioxidant systems to defend tissues from pro-oxidants is well recognized (Thomas, 1995). GSH is non-enzymatic, whereas SOD, CAT, and GPx are enzymatic endogenous antioxidants (Flora et al., 2012). Another significant conclusion of the current study was that AA therapy causes a drop in the tissue levels of SOD, CAT, and GPx. These results are consistent with the previous study that showed AA-induced colitis to have impaired antioxidant mechanisms and enhanced LPO (Nieto et al., 2000). The TAC level was decreased in AA, while the protection with a high dose has increased significantly, this is consistent with the results of the previous studies (Ermiş et al., 2013; Cagin et al., 2016). The results of the current investigation showed that administering the extract orally to rats with AA-induced colitis might lessen the severity of the colonic mucosal injury, stop the rise in MDA levels, and replenish depleted levels of antioxidant enzyme activities. Therefore, the extract is more efficient when given after colitis has been induced in a dose-dependent manner. The findings revealed that extract significantly and dose-dependently reduced both carrageenan-induced hind paw edema and cotton-pellet granuloma (Gobianand et al., 2010).

Numerous plant species, including, *Moringa oleifera* (Minaiyan et al., 2014), *Coriandrum sativum* (Heidari et al., 2016), and *Helichrysum oligocephalum* (Popov et al., 2006), have had protective effects on colonic tissues against UC examined. However, there aren't many publications examining the impact of *C. fistula*. The pathological analysis supported the biochemical changes. The detected histological alternation, such as clogged blood arteries, leukocytic infiltration, and various degrees of cell degeneration, were consistent with prior studies of UC by other authors (Tanide et al., 2014; 2016).

The present investigation is in parallel with the study of Zabihi et al. (2024) that revealed the extract from the *C. fistula* plant has beneficial effects on the healing process of ulcerative colitis, demonstrating a reduction in colitis symptoms. Particularly, the composition of the aqueous extract proved effective in diminishing the activity of the myeloperoxidase (MPO) enzyme when compared to the control group. These findings suggest a potential therapeutic role for *C. fistula* in managing ulcerative colitis by mitigating inflammation and influencing specific enzyme activity involved in the condition as well as controlling the oxidative/antioxidant balance. Zabihi et al. (2024) used high doses with short time; 600 and 800 mg/kg once daily for 5 days.

3.4.6. Histological evaluation

Colonic mucosa from the control group was shown by H&E-stained sections to be made up of densely aggregated simple tubular glands (Lieberkuhn crypts), which extended down to the muscularis mucosa and were embedded in the lamina propria. The crypts' lining was made up mostly of numerous goblet cells and surface epithelial columnar absorptive cells with an apical brush border and basal oval nuclei. Basal nuclei and vacuolated cytoplasm were visible in goblet cells. A small number of intraepithelial lymphocytes were also visible. Undifferentiated cells with basal oval vesicular nuclei were present in the basal regions of the crypts (Fig. 5A). In the positive control group, staining revealed focal areas of severe mucosal deformation, exfoliation, and ulceration with loss of the whole crypt lining in the acetic acid-induced

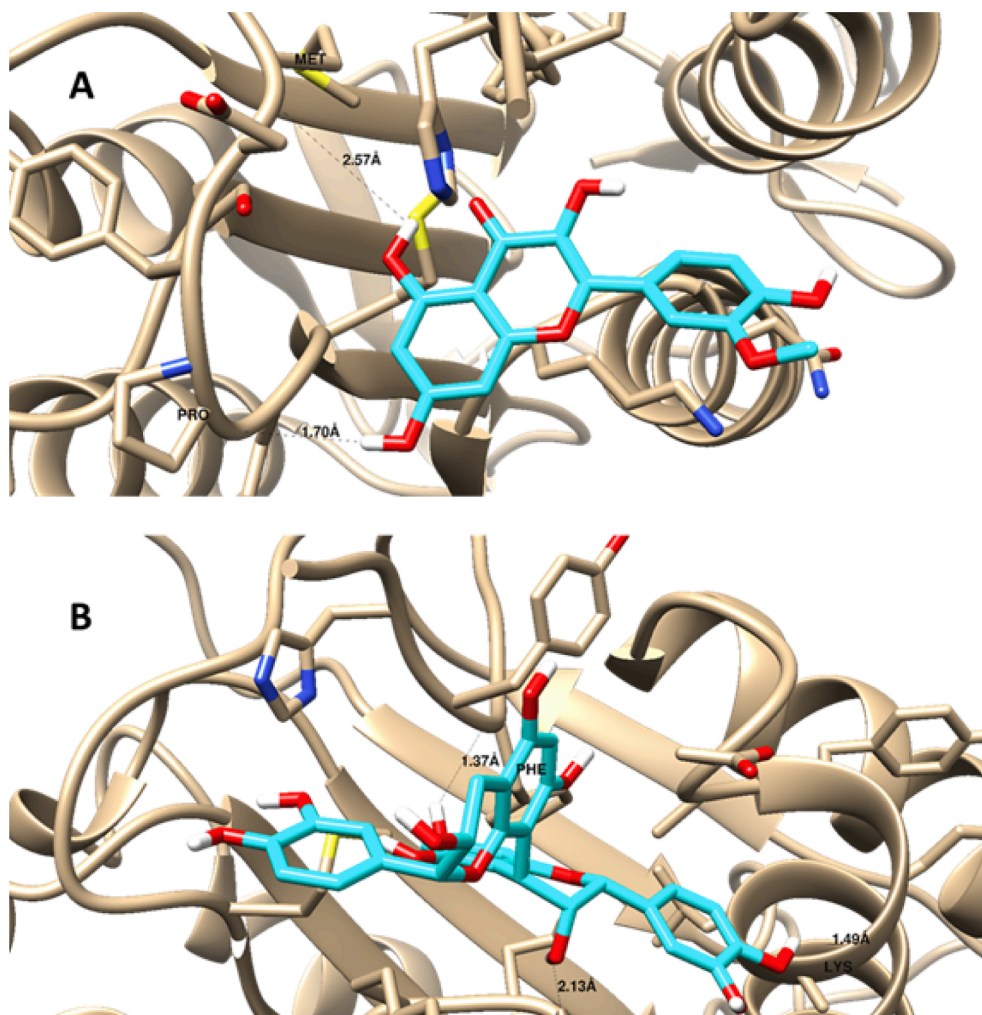


Fig. 10. Ligand-disposition and receptor interactions of A) Isorhamnetin and B) Procyanidin B2 inside Caspase-3 protein demonstrating a surface representation. 3D images were made by Chimera software.

UC group. Some crypts displayed dilatation along with a notable reduction in goblet cells or their disappearance. Transmural necrosis, edoema, and diffuse inflammatory cell infiltration in the mucosa were histological features of untreated rats. Desquamated regions, loss of the epithelium, and focal ulceration of the colonic mucosa that penetrated the muscularis mucosa were present. Hyperplasia of the crypt cells and shorter crypt cell lengths are signs of malabsorption. Tubular adenomas are present along with hyperplastic colorectal polyps (hyperplastic polyposis) in (Fig. 5B).

The degree and severity of the histological signs of cell damage were considerably decreased in the sulfasalazine-treated group. The lamina propria had a few mildly inflammatory cells, but the epithelium was undamaged. However, sulfasalazine reduced microscopic harm and preserved the normal alignment of cell structure. Lieberkühn's goblet cells and crypts were both discernible and well-spaced. Reduced leukocytosis was seen (Fig. 5C). The prophylactic low dose (200 mg/kg/day) group's histological characteristics included necrosis of a few crypts and a moderate inflammatory response in the mucosa and submucosa (Fig. 5D). Fig. 5E showed pseudo-Peyer's patches without any discernible polyps. The mucosa deteriorated and infiltrated with fewer inflammatory cells in the preventative group, which received a high dose (400 mg/kg/day), than in the protection group which received a low dose. With the growth of multiple goblet cells, crypt cells grew larger. Polyps cannot be seen. little inflammation without any signs of tissue damage in the mucosa and submucosa. Additionally, crypts displayed a typical architectural design with complete vacuolated goblet

cells.

The treatment groups showed desquamated regions and epithelium loss after receiving a lower dose (200 mg/kg/day) of *C. fistula*. With many increases in the quantity and total degeneration of goblet cells, the crypt architecture was also altered. Inflammatory cells had invaded the lamina propria with no evidence of polyps (Fig. 5F). However, higher-dose therapy (400 mg/kg/day) improved microscopic damage and preserved the regular organization of cell structure. Lieberkühn's goblet cells and crypts were both distinct and evenly spaced. Infiltration and necrosis were diminished (Fig. 5G).

Rats given a high dose of MLE showed normal epithelium on their surface and only a small amount of inflammatory cells were infused. Animals administered the extract as treatment were protected against the AA's effects of inflammation, congestion, ulceration, erosion, necrosis, and hyperplasia. The complete colonic mucosa's cytoarchitecture was also preserved. This demonstrates the extract's capacity to safeguard the animals and slow the spread of the illness. The treated animals had better healing than the protective male rats.

3.4.7. Immunohistochemically evaluation

As seen in the figures, several cells in the negative control group had a mildly positive cytoplasmic COX2 immuno-histochemical reaction, which was manifested as a brownish color (Fig. 6A). However, sections taken from group II showed many cells with a high positive cytoplasmic COX2 reaction (Fig. 6B). The section from group III, on the other hand, had several cells that had a positive cytoplasmic COX2 reaction

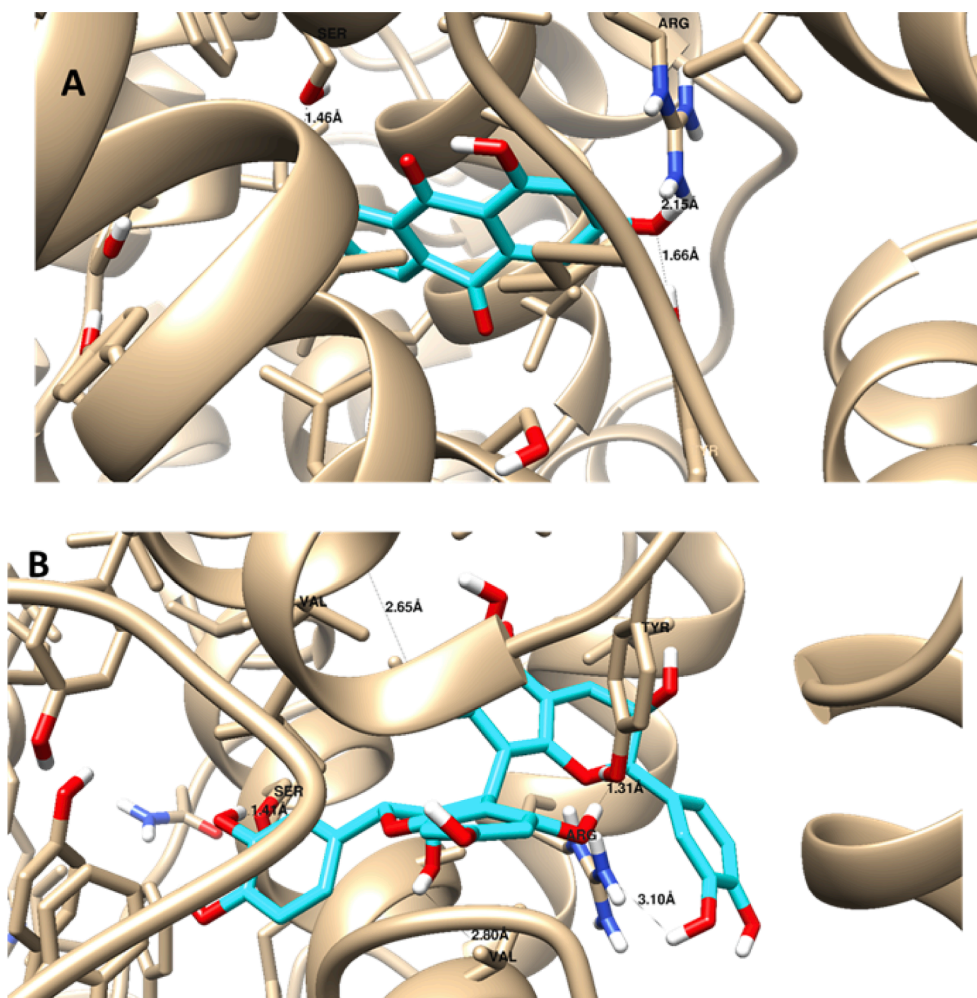


Fig. 11. Ligand disposition and receptor interactions of A) Emodin and B) Procyanidin B2 inside COX-2 protein demonstrating a surface representation. 3D images were made by Chimera software.

(Fig. 6C). Sections from groups IV and VI, however, revealed a few cells with a slightly positive COX2 reaction in the cytoplasm (Fig. 6D and 6E). Sections from groups V and VII displayed a COX2 reaction that was almost normal (Fig. 6F and 6G). Meanwhile, immuno-stained sections from the control group showed a few cells with a weakly positive cytoplasmic caspase-3 immuno-histochemical reaction, shown as a brownish coloring (Fig. 7A). However, the group II section showed several cells with a markedly positive caspase-3 reaction (Fig. 7B). Additionally, a few cells in the group III section had a weakly positive caspase-3 reaction (Fig. 7C). A mildly positive caspase-3 reaction was seen in several cells in sections from groups IV and VI (Fig. 7D and 7E). Sections from groups V and VII, on the other hand, displayed a nearly typical caspase-3 response (Fig. 7F and 7G).

Image J software (version 1.53 h) was used for morphometric analysis to semi-quantify COX-2 and Caspase -3 reactivity in the analyzed tissues. Following Fig. 8, when compared to the control group, group II showed a highly significant rise in the mean percentage area of positive COX-2 reactivity. In contrast to the AA-induced colitis, sulfasalazine, and low *C. fistula*-treated groups, group VII showed a considerable decline. When compared to the AA-induced group, a substantial reduction was also seen in groups III, IV, V, and VI. On the other hand, group II showed a highly significant increase in the mean percentage of positive caspase-3 reaction when compared to the control group. Group VII among the II, III, and VI groups showed a notable improvement in the mean percentage area. Comparing Groups III, IV, and V to the AA-induced UC group, there was a noticeable decline. Group VI and the

AA-induced UC rats, however, showed no statistically significant difference (Fig. 9).

The colonic caspase-3 and COX-2 activity of the AA group was higher than that of the control group concerning the inflammatory response. A highly substantial rise in group AA when compared to the control group was revealed by morphometrical analysis of the mean percentage of positive caspase-3 and COX-2 reaction, which confirmed this. Improvement in the mean percentage area was remarkable in the treated group with a high dose of MLE amongst the AA, sulfasalazine-treated, and treated group with a low dose.

3.5. Molecular docking

Using molecular docking simulation, the chemicals found by LC/MS/MS in this investigation were tested against the COX-2 and caspase-3 proteins. As can be observed in Tables 9 and 10, the majority of the compounds under investigation demonstrated strong binding affinities to the two proteins, with binding energies of -3.4 to -15.26 Kcal/mol and -5.8 to -16.25 Kcal/mol, respectively, towards the COX-2 and caspase-3 proteins. In addition, these compounds had noticeable molecular interactions with the key amino acids; His 121 and Arg 207 inside caspase-3, as well as Tyr 355 and Arg 120 inside COX-2 protein. Isorhamnetin exhibited the highest affinity, indicated by its low docking score value (-19.4 Kcal/mol) and the best ligand-receptor interaction to caspase-3 proteins (1 Arene-arene with His 121 and 2 HB; one with His 121 and the other one with Arg 207)

On the other hand, emodin displayed the best interaction with COX-2. Since its docking score value (-13.2Kcal/mol) and the best ligand-receptor interaction to COX-2 protein (it formed 3 HB; 2 HB with Ile 12 and 1HB with Asp 15)

Procyanidin B2, one of the top interacting compounds, demonstrated significance towards both proteins. It exhibited a docking score value of -16.25Kcal/mol and formed 1HB with Arg 207, 1HB with His 121, and an Arene-cation His 121 the key amino acids in the active site of caspase-3 protein. It exhibited binding energy of -15.26 Kcal/mol and formed 1 HB with Ile 12, 1 HB with Asp 15, and 1 Arene-cation His 13, the crucial amino acids in the target protein that represent the essential residues in the binding of isorhamnetin, procyanidin B2 towards caspase-3 protein and emodin, procyanidin B2 towards COX-2 protein were highlighted in Figs. 10 and 11, respectively.

Docking studies revealed that most of the identified compounds in *C. fistula* displayed good binding affinities towards the target proteins; caspase-3 and COX-2 where isorhamnetin was the most interactive compound with caspase-3. Emodin was the best compound to bind with COX-2 and procyanidin B2 which had strong dual affinity to both investigated proteins. These results supported the experimental ones given the antiapoptotic and anti-inflammatory effects of *C. fistula* that were mediated by caspase-3 and COX-2 inhibition, respectively. Furthermore, our docking finding matched with the literature regarding the antiapoptotic effects of isorhamnetin, since it reversed H₂O₂-induced apoptotic damage in H9c2 cardiomyocytes. It also reduced atherosclerosis in animals and shielded human brain microvascular endothelial cells from methylglyoxal- and oxygen-glucose-induced cytotoxicity. These protective actions were mediated by caspase-3 inactivation (Sun et al., 2012; Luo et al., 2015; Li et al., 2016). On the other side, the COX-2 inhibition effect of emodin was reported in earlier studies. Emodin attenuated neuropathy induced by oxaliplatin through the inhibition of spinal inflammation mediated by COX2/NF- κ B (Yang et al., 2023) Also, this anthraquinone suppressed inflammation and development and progression of cancer in intestinal carcinogenesis associated with AOM/DSS-triggered colitis (Zhang et al., 2021) Furthermore, emodin reduced rheumatoid arthritis procession by the reduction of plasma levels of TNF- α and IL-6 as well as downregulation of COX-2 protein expression in synovial tissue resulting in decreased production of PGE (2) (Stompor-Gorący, 2021; Cheng et al., 2022). Besides, the COX-2 and caspase-3 inhibition activities of procyanidin B2 were evidenced (Yang et al., 2015; Song et al., 2021; Cai et al., 2022).

4. Conclusion

This comprehensive investigation aimed to shed light on the antioxidant properties and potential therapeutic effects of *C. fistula* leaves. The study findings highlight the richness of *C. fistula* leaves in phenolic compounds, particularly flavonoids, as indicated by total phenolic content (TPC), total flavonoid content (TFC), and LC/MS/MS analysis. The research underscores the *in vitro* antioxidant potential of *C. fistula*, demonstrated through free radical quenching, Fe³⁺ ions reduction, and pho-molybdenum assay. Moreover, the study evaluates the therapeutic potential of *C. fistula* (either as treatment or protectant) against acetic acid-induced ulcerative colitis, showing that the plant extract, especially in crude form, mitigates injuries and restores hematological and biochemical parameters, especially when used as treatment rather than as a protectant. It ameliorates histopathological lesions, prevents reactive oxygen species (ROS) overproduction, and downregulates inflammatory and apoptosis markers (COX-2 and caspase-3). The research suggests the need for further investigations to develop pharmaceutical formulations of *C. fistula* and conduct clinical trials to assess its therapeutic potential in ulcerative colitis patients.

Funding

This research received no external funding

Institutional Review Board Statement:

The study was conducted by the Declaration of Helsinki and approved by the Ethics Committee of FACULTY OF PHARMACY, SUEZ CANAL UNIVERSITY (NO. 202005 M1).

Acknowledgments

The authors would like to acknowledge Dr. Heba Nageh Gad El-Hak, Assistant Professor of Histology, Zoology Department, Faculty of Science, Suez Canal University, for histochemical and immunohistochemical results interpretation.

Appendix A. Supplementary data

Supplementary data to this article can be found online at <https://doi.org/10.1016/j.arabjc.2024.105672>.

References

- Aabideen, Z.U., Mumtaz, M.W., Akhtar, M.T., Raza, M.A., Mukhtar, H., Irfan, A., Raza, S.A., Touqeer, T., Nadeem, M., Saari, N., 2021. *Cassia fistula* Leaves, UHPLC-QTOF-MS/MS based metabolite profiling, and molecular docking insights to explore bioactives role towards inhibition of pancreatic Lipase. *Plants* 10 (7), 1334. <https://doi.org/10.3390/plants10071334>.
- Abbas, H.A., Salama, A.M., El-Toumy, S.A.A., Salama, A.A., Tadros, S.H., El Gedaily, R.A., 2022. Novel neuroprotective potential of *Bunchosia armeniaca* (Cav.) DC against lipopolysaccharide induced Alzheimer's disease in mice. *Plants* 11 (14), 1792. <https://doi.org/10.3390/plants11141792>.
- Abd Ghafar, S.Z., Mediani, A., Ramli, N.S., Abas, F., 2018. Antioxidant, α -glucosidase, and nitric oxide inhibitory activities of *Phyllanthus* acids and LC-MS/MS profile of the active extract. *Food Biosci.* 25, 134–140. <https://doi.org/10.1016/j.fbio.2018.08.009>.
- Abdallah, H.M.I., Ammar, N.M., Abdelhameed, M.F., Gendy, A.-E.-N.-G.-E., Ragab, T.I. M., Abd-ElGawad, A.M., Farag, M.A., Alwahibi, M.S., Elshamy, A.I., 2020. Protective mechanism of *acacia saligna* butanol extract and its nano-formulations against ulcerative colitis in rats as revealed via biochemical and metabolomic assays. *Biology* 9 (8), 195. <https://doi.org/10.3390/biology9080195>.
- Abdel, M.T., 2021. Cytotoxic potentials and phytoconstituents profiling of *Blepharis edulis* (Forsk.) Pers. Using UHplc/q-ToF-Ms-Ms. *Al-Azhar J. Pharm. Sci.* 63, 37–56. <https://doi.org/10.21608/ajps.2021.153559>.
- Abdelhameed, R.F., Elhady, S.S., Sirwi, A., Samir, H., Ibrahim, E.A., Thomford, A.K., El Gindy, A., Hadad, G.M., Badr, J.M., Nafie, M.S., 2021. *Thonningia sanguinea* extract: antioxidant and cytotoxic activities supported by chemical composition and molecular docking simulations. *Plants* 10 (10), 2156. <https://doi.org/10.3390/plants10102156>.
- Abo-Elghiet, F., Ibrahim, M.H., El Hassab, M.A., Bader, A., Abdallah, Q.M., Temraz, A., 2022. LC/MS analysis of *Viscum cruciatum* Sieber ex Boiss. extract with antiproliferative activity against MCF-7 cell line via G0/G1 cell cycle arrest: An *in-silico* and *in-vitro* study. *J. Ethnopharmacol.* 295, 115439 <https://doi.org/10.1016/j.jep.2022.115439>.
- Abraham, B.P., Ahmed, T., Ali, T., 2017. Inflammatory bowel disease: pathophysiology and current therapeutic approaches. *Handb. Exp. Pharmacol.* 239, 115–146.
- Aebi, H., 1984. Catalase *in vitro*. *Methods Enzymol.* 105, 121–126.
- Ahmed, M.M., Zaki, N.I., 2009. Assessment the ameliorative effect of pomegranate and rutin on chlorpyrifos-ethyl-induced oxidative stress in rats. *Nature Sci.* 7, 49–61.
- Alhawarri, M.B., Dianita, R., Rawa, M.S.A., Nogawa, T., Wahab, H.A., 2023. Potential anti-cholinesterase activity of bioactive compounds extracted from *Cassia grandis* L.f. and *Cassia timoriensis* DC. *Plants* 12 (2), 344. <https://doi.org/10.3390/plants12020344>.
- Ali, M.A., 2014. *Cassia fistula* Linn: a review of phytochemical and pharmacological studies. *Int J Pharm Sci Res* 5 (6), 2125–2130.
- Alia, F., Syamsunarno, M.R.A.A., Sumirat, V.A., Ghazali, M., Atik, N., 2019. The hematological profiles of high-fat diet mice model with *moringa oleifera* leaves ethanolic extract treatment. *Biomed. Pharmacol. J.* 12, 2143–2149. <https://doi.org/10.13005/bpj/1849>.
- Al-Rejaie, S.S., Abuhashish, H.M., Ahmed, M.M., Aleisa, A.M., Alkhamees, O., 2012. Possible biochemical effects following inhibition of ethanol-induced gastric mucosa damage by *Gymnema sylvestre* in male Wistar albino rats. *Pharm. Biol. (abingdon, U. K.)* 50, 1542–1550. <https://doi.org/10.3109/13880209.2012.694894>.
- Alsharif, I.A., Fayed, H.M., Abdel-Rahman, R.F., Abd-El salam, R.M., Ogaly, H.A., 2022. Miconazole Mitigates acetic acid-induced experimental colitis in rats: insight into inflammation, oxidative stress, and keap1/nrf-2 signaling crosstalk. *Biology* 11 (2), 303. <https://doi.org/10.3390/biology11020303>.
- Anlas, C., Bakirel, T., Ustuner, O., Ustun-Alkan, F., Diren-Sigirci, B., Koca-Caliskan, U., Mancak-Karakus, M., Dogan, U., Ak, S., Akpulat, H.A., 2023. In vitro biological activities and preliminary phytochemical screening of different extracts from *Achillea sintenisii* Hub-Mor. *Arabian J. Chem.* 16 (1), 104426 <https://doi.org/10.1016/j.arabjc.2022.104426>.
- Attallah, N.G.M., El-Kadem, A.H., Negm, W.A., Elekhaway, E., El-Masry, T.A., Elmongy, E.I., Altwajry, N., Alanazi, A.S., Al-Hamoud, G.A., Ragab, A.E., 2021.

- Promising antiviral activity of agrimonia pilosa phytochemicals against severe acute respiratory syndrome coronavirus 2 supported with *in vivo* mice study. *Pharmaceu.* 14 (12), 1313. <https://doi.org/10.3390/ph14121313>.
- Autor, E., Cornejo, A., Bimbela, F., Maisterra, M., Gandia, L.M., Martínez-Merino, V., 2022. Extraction of phenolic compounds from *Populus Salicaceae* bark. *Biomolecules* 12 (4), 539. <https://doi.org/10.3390/biom12040539>.
- Awaad, A.S., Alafeefy, A.M., Alasmay, F.A.S., El-Meligy, R.M., Alqasoumi, S.I., 2017. Anti-ulcerogenic and anti-ulcerative colitis (UC) activities of seven amines derivatives. *Saudi Pharm. J.* 25, 1125–1129. <https://doi.org/10.1016/j.jsps.2017.07.003>.
- Bastaki, S.M.A., Amir, N., Adeghate, E., Ojha, S., 2022. Lycopodium mitigates oxidative stress and inflammation in the colonic mucosa of acetic acid-induced colitis in rats. *Molecules* 27 (9), 2774. <https://doi.org/10.3390/molecules27092774>.
- Bhakta, T., Mukherjee, P.K., Saha, K., Pal, M., Saha, B.P., 1999. Evaluation of anti-inflammatory effects of *Cassia fistula* (Leguminosae) leaf extracts on rats. *J Herbs Spices Med Plants.* 6, 67–72. https://doi.org/10.1300/J044v06n04_08.
- Brito, A., Ramirez, J.E., Areche, C., Sepúlveda, B., Simirgiotis, M.J., 2014. HPLC-UV-MS profiles of phenolic compounds and antioxidant activity of fruits from three citrus species consumed in Northern Chile. *Molecules* 19 (11), 17400–17421. <https://doi.org/10.3390/molecules191117400>.
- Cagin, Y.F., Parlakpinar, H., Vardi, N., Polat, A., Atayan, Y., Erdogan, M.A., Tanbek, K., 2016. Effects of dexpanthenol on acetic acid-induced colitis in rats. *Exp. Ther. Med.* 12, 2958–2964. <https://doi.org/10.3892/etm.2016.3728>.
- Cai, W., Zhang, Y., Jin, W., Wei, S., Chen, J., Zhong, C., Zhong, Y., Tu, C., Peng, H., 2022. Procyandin B2 ameliorates the progression of osteoarthritis: An *in vitro* and *in vivo* study. *Int. Immunopharmacol.* 113, 109336 <https://doi.org/10.1016/j.intimp.2022.109336>.
- Chang, J.-F., Yeh, J.-C., Ho, C.-T., Liu, S.-H., Hsieh, C.-Y., Wang, T.-M., Chang, S.-W., Lee, I.-T., Huang, K.-Y., Wang, J.-Y., Lin, W.-N., 2019. Targeting ROS and cPLA2/COX2 expressions ameliorated renal damage in obese mice with endotoxemia. *Int. J. Mol. Sci.* 20 (18), 4393. <https://doi.org/10.3390/ijms20184393>.
- Chen, G.-L., Munyao Mutie, F., Xu, Y.-B., Saleri, F.D., Hu, G.-W., Guo, M.-Q., 2020. Antioxidant, anti-inflammatory activities and polyphenol profile of *Rhamnus prinoides*. *Pharmaceuticals* 13 (4), 55. <https://doi.org/10.3390/ph13040055>.
- Cheng, L., Chen, J., Rong, X., 2022. Mechanism of emodin in the treatment of rheumatoid arthritis. *Evid. Based Complement. Alternat. Med.* ID 9482570.
- Chou, O., Ali, A., Subbiah, V., Barrow, C.J., Dunshea, F.R., Suleria, H.A.R., 2021. LC-ESI-QTOF-MS/MS characterisation of phenolics in herbal tea infusion and their antioxidant potential. *Fermentation* 7 (2), 73. <https://doi.org/10.3390/fermentation7020073>.
- Costa Silva, T.D., Justino, A.B., Prado, D., Koch, G., Martins, M.M., Santos, P.S., Morais, S.A., Goulart, L.R., Cunha, L.C., Sousa, R.M., Espíndola, F.S., de Oliveira, A., 2019. Chemical composition, antioxidant activity, and inhibitory capacity of α -amylase, α -glucosidase, lipase, and non-enzymatic glycation, *in vitro*, of the leaves of *Cassia bakeriana* Craib. *Ind. Crops Prod.* 140, 111641 <https://doi.org/10.1016/j.indcrop.2019.111641>.
- Das, N., Islam, M.E., Jahan, N., Islam, M.S., Khan, A., Islam, M.R., Parvin, M.S., 2014. Antioxidant activities of ethanolic extracts and fractions of *Crescentia cujete* leaves and stem bark and the involvement of phenolic compounds. *BMC Complementary Altern. Med.* 14, 45.
- Djeridane, A., Yousfi, M., Nadjemi, B., Boutassoua, D., Stocker, P., Vidal, N., 2020. Antioxidant activity of some Algerian medicinal plants extracts containing Phenolic compounds. *Food Chem.* 97 (4), 654–660. <https://doi.org/10.1016/j.foodchem.2005.04.028>.
- Dothel, G., Vasina, V., Barbara, G., De Ponti, F., 2013. Animal models of chemically induced intestinal inflammation: predictivity and ethical issues. *Pharmacol. Ther.* 139, 71–86. <https://doi.org/10.1016/j.pharmthera.2013.04.005>.
- El-Abhar, H.S., Hammad, L.N., Gawad, H.S.A., 2008. Modulating effect of ginger extract on rats with ulcerative colitis. *J. Ethnopharmacol.* 118, 367–372. <https://doi.org/10.1016/j.jep.2008.04.026>.
- Elhady, S.S., Abdelhameed, R.F.A., Mehanna, E.T., Wahba, A.S., Elfaky, M.A., Koshak, A. E., Noor, A.O., Bogari, H.A., Malatani, R.T., Goda, M.S., 2022. Metabolic profiling, chemical composition, antioxidant capacity, and *in vivo* hepato- and nephroprotective effects of *sonchus cornutus* in mice exposed to cisplatin. *Antioxidants* 11 (5), 819. <https://doi.org/10.3390/antiox11050819>.
- El-Hawary, S.S., Hammam, W.E., El-Tantawi, M.E., Yassin, N.A., Kirolos, F.N., Abdelhameed, M.F., Abdelfattah, M.A., Wink, M., Sobeh, M., 2021. Apple leaves and their major secondary metabolite phlorizin exhibit distinct neuroprotective activities: Evidence from *in vivo* and *in silico* studies. *Arabian J. Chem.* 14 (6), 103188 <https://doi.org/10.1016/j.arabjc.2021.103188>.
- Elmongy, E.I., Negm, W.A., Elekhawy, E., El-Masry, T.A., Attallah, N.G., Altwaijry, N., Batiha, G.E., El-Sherbeni, S.A., 2022. Anti-diarrheal and antibacterial activities of *Monterey cypress* phytochemicals: *in vivo* and *in vitro* approach. *Molecules* 27 (2), 346. <https://doi.org/10.3390/molecules27020346>.
- El-Shenawy, N., Abdel-Nabi, L., Abdel, N., 2006. Hypoglycemic effect of *Cleome droserifolia* ethanolic leaf extract in experimental diabetes, and on non-enzymatic antioxidant, glycogen, thyroid hormone, and insulin levels. *Diabetol. Croat.* 28, 35–41.
- Eltamany, E.E., Elhady, S.S., Ahmed, H.A., Badr, J.M., Noor, A.O., Ahmed, S.A., Nafie, M. S., 2020. Chemical profiling, antioxidant, cytotoxic activities and molecular docking simulation of *Carrichtera annua* DC. (cruciferae). *Antioxidants* 9 (12), 1286. <https://doi.org/10.3390/antiox9121286>.
- Eltamany, E.E., Elhady, S.S., Nafie, M.S., Ahmed, H.A., Abo-Elmatty, D.M., Ahmed, S.A., Badr, J.M., Abdel-Hamed, A.R., 2021. The Antioxidant *Carrichtera annua* DC. ethanolic extract counteracts cisplatin-triggered hepatic and renal toxicities. *Antioxidants* 10 (6), 825. <https://doi.org/10.3390/antiox10060825>.
- Eltamany, E.E., Goda, M.S., Nafie, M.S., Abu-Elsaoud, A.M., Hareeri, R.H., Aldurduj, M. M., Elhady, S.S., Badr, J.M., Eltahawy, N.A., 2022. Comparative assessment of the antioxidant and anticancer activities of *Plicosepalus acacia* and *Plicosepalus curviflorus*: Metabolomic profiling and *in silico* Studies. *Antioxidants* 11 (7), 1249. <https://doi.org/10.3390/antiox11071249>.
- Ermis, H., Parlakpinar, H., Gulbas, G., Vardi, N., Polat, A., Cetin, A., Kilic, T., Aytemur, Z. A., 2013. Protective effect of dexpanthenol on bleomycin-induced pulmonary fibrosis in rats. *Naunyn-Schmiedeberg's Arch. Pharmacol.* 386, 1103–1110.
- Fan, Y., Li, Y., Wu, Y., Li, L., Wang, Y., Li, Y., 2017. Identification of the chemical constituents in *Simiao wan* and rat plasma after oral administration by GC-MS and LC-MS. *Evidence-Based Complement. Altern. Med.*
- Flora, G., Gupta, D., Tiwari, A., 2012. Toxicity of lead: a review with recent updates. *Interdiscip. Toxicol.* 5, 47. <https://doi.org/10.2478/v10102-012-0009-2>.
- Fu, Z.W., Li, Z.X., Hu, P., Feng, Q., Xue, R., Hu, Y.Y., Huang, C.G., 2015. A practical method for the rapid detection and structural characterization of major constituents from traditional Chinese medical formulas: analysis of multiple constituents in *Yinchenhao* decoction. *Anal. Methods* 7 (11), 4678–4690.
- Gobianand, K., Vivekanandan, P., Pradeep, K., Mohan, C.V.R., Karthikeyan, S., 2010. Anti-inflammatory and Antipyretic Activities of Indian Medicinal Plant *Cassia fistula* Linn. (Golden Shower) in Wistar Albino Rats. *Int. J. Pharmacol.* 6, 719–725.
- Goda, M.S., Nafie, M.S., Awad, B.M., Abdel-Kader, M.S., Ibrahim, A.K., Badr, J.M., Eltamany, E.E., 2022. *In vitro* and *in vivo* studies of anti-lung cancer activity of *Artemisia judaica* L. crude extract combined with LC-MS/MS metabolic profiling, docking simulation, and HPLC-DAD quantification. *Antioxidants* 11 (1), 17. <https://doi.org/10.3390/antiox11010017>.
- Gornall, A.G., 1949. Determination of serum proteins by means of the biuret reactions. *J. Biol. Chem.* 177, 51.
- Goufo, P., Singh, R.K., Cortez, I., 2020. A Reference list of phenolic compounds (including stilbenes) in grapevine (*Vitis vinifera* L.) roots, woods, canes, stems, and leaves. *Antioxidants* 9 (5), 398. <https://doi.org/10.3390/antiox9050398>.
- Hagar, H.H., El-Medany, A., El-Eter, E., Arafa, M., 2007. Ameliorative effect of pyrrolidinedithiocarbamate on acetic acid-induced colitis in rats. *Eur. J. Pharmacol.* 554, 69–77.
- Hasona, N., Hussien, T., 2017. Biochemical, histopathological, and histochemical effects of *Vitis vinifera* L extract on acetic acid-induced colitis. *J. Complementary Med. Res.* 6, 351.
- Hegazy, M.M., Afifi, W.M., Metwaly, A.M., Radwan, M.M., Abd-Elraouf, M., Mehany, A. B.M., Ahmed, E., Enany, S., Ezzeldin, S., Ibrahim, A.E., El Deeb, S., Mostafa, A.E., 2022. Antitrypanosomal, anti topoisomerase-I, and cytotoxic biological evaluation of some African plants belonging to Crassulaceae, chemical profiling of extract using UHPLC/QTOF-MS/MS. *Molecules* 27 (24), 8809. <https://doi.org/10.3390/molecules27248809>.
- Heidari, B., Sajjadi, S.E., Minaian, M., 2016. Effect of *Coriandrum sativum* hydroalcoholic extract and its essential oil on acetic acid-induced acute colitis in rats. *Avicenna J. Phytomed.* 6, 205–214.
- Hu, J., Qi, Q., Zhu, Y., Wen, C., Olatunji, O.J., Jayeoye, T.J., Eze, F.N., 2023. Unveiling the anticancer, antimicrobial, antioxidative properties, and UPLC-ESI-QTOF-MS/GC-MS metabolite profile of the lipophilic extract of siam weed (*Chromolaena odorata*). *Arabian J. Chem.* 16 (7), 104834 <https://doi.org/10.1016/j.arabjc.2023.104834>.
- Kanwal, A., Azeem, F., Nadeem, H., Ashfaq, U.A., Aadil, R.M., Kober, A.K.M.H., Rajoka, M.S.R., Rasul, I., 2022. molecular mechanisms of *Cassia fistula* against epithelial ovarian cancer using network pharmacology and molecular docking approaches. *Pharmaceutics* 14 (9), 1970. <https://doi.org/10.3390/pharmaceutics14091970>.
- Karar, M.E., Kuhnert, N.J., 2015. UPLC-ESI-Q-TOF-MS/MS characterization of phenolics from *Crataegus monogyna* and *Crataegus laevigata* (Hawthorn) leaves, fruits, and their herbal derived drops (Crataegut Tropfen). *J. Chem. Biol. Therap.* 1, 102. <https://doi.org/10.4172/2572-0406.1000102>.
- Kaur, S., Kumar, A., Thakur, S., Kumar, K., Sharma, R., Sharma, A., Singh, P., Sharma, U., Kumar, S., Landi, M., Brestić, M., Kaur, S., 2020. Antioxidant, antiproliferative, and apoptosis-inducing efficacy of fractions from *Cassia fistula* L. leaves. *Antioxidants* 9 (2), 173. <https://doi.org/10.3390/antiox9020173>.
- Keshavarzi, Z., Nurmohammadi, F., Majlesi, S., Maghool, F., 2019. Protective effects of walnut extract against oxidative damage in acetic acid-induced experimental colitis rats. *Physiol. Pharmacol.* 23, 51–58. <http://eprints.mui.ac.ir/id/eprint/10161>.
- Khan, B.A., Akhtar, N., Rasul, A., Mahmood, T., Khan, H.S., Iqbal, M., Murtaza, G., 2012. Investigation of the effects of extraction solvent/technique on the antioxidant activity of *Cassia fistula* L. *J. Medic. Plants Res.* 6 (3), 500–503. <https://doi.org/10.5897/JMPR11.1289>.
- Khurmi, M., Wang, X., Zhang, H., Hussain, S.N., Qaisar, M.N., Hayat, K., Saqib, F., Zhang, X., Zhan, G., Guo, Z., 2021. The genus *Cassia* L.: Ethnopharmacological and phytochemical overview. *Phytotherapy Res.* 35 (5), 2336–2385. <https://doi.org/10.1002/ptr.6954>.
- Kishk, S.M., Kishk, R.M., Yassen, A.S.A., Nafie, M.S., Nembr, N.A., ElMasry, G., Al-Rejaie, S., Simons, C., 2020. Molecular insights into human transmembrane protease serine-2 (TMP2) inhibitors against SARS-CoV2: Homology modeling, molecular dynamics, and docking studies. *Molecules* 25 (21), 5007. <https://doi.org/10.3390/molecules25215007>.
- Kishk, S.M., Eltamany, E.E., Nafie, M.S., Kinkar, R.M., Hareeri, R.H., Elhady, S.S., Yassen, A.S.A., 2022. Design and synthesis of coumarin derivatives as cytotoxic agents through PI3K/AKT Signaling pathway inhibition in HL60 and HepG2 cancer cells. *Molecules* 27 (19), 6709. <https://doi.org/10.3390/molecules27196709>.
- Kusumaningtyas, V., Juliawaty, L., Syah, Y., 2020. Two stilbenes from Indonesian *Cassia grandis* and their antibacterial activities. *Res. J. Chem. Environ.* 24, 61–63.

- Kwon, K.H., Murakami, A., Tanaka, T., Ohgashi, H., 2005. Dietary rutin, but not its aglycone quercetin, ameliorates dextran sulfate sodium-induced experimental colitis in mice: attenuation of pro-inflammatory gene expression. *Biochem. Pharmacol.* (Amsterdam, Neth.). 69, 395–406. <https://doi.org/10.1016/j.bcp.2004.10.015>.
- Laxmi, V., Bhatia, A.K., Goel, A., Wahi, N., Sharma, A., 2015. Phytochemicals screening and analysis using HPLC to determine the antimicrobial efficacy of *Cassia fistula* extract. *Adv. Bio Res.* 2015 (6), 1–7. <http://www.soeagra.com/abr.html>.
- Li, W., Chen, Z., Yan, M., He, P., Chen, Z., Dai, H., 2016. The protective role of isorhamnetin on human brain microvascular endothelial cells from cytotoxicity induced by methylglyoxal and oxygen-glucose deprivation. *J. Neurochem.* 136, 651–659. <https://doi.org/10.1111/jnc.13436>.
- Lin, Q., Li, Y., Tan, X.M., Yao, X.C., 2013. Simultaneous determination of formononetin, calycosin, and isorhamnetin from *Astragalus mongholicus* in rat plasma by LC-MS/MS and application to pharmacokinetic study. *Zhong Yao Cai* 36, 589–593.
- Luo, Y., Sun, G., Dong, X., Wang, M., Qin, M., Yu, Y., Sun, X., 2015. Isorhamnetin attenuates atherosclerosis by inhibiting macrophage apoptosis via PI3K/AKT activation and HO-1 induction. *PLoS One* 10, e0120259.
- MassBank. Available online: <https://massbank.eu/MassBank/> (accessed on 12 April 2023).
- Minaiyan, M., Asghari, G., Taheri, D., Saeidi, M., Nasr-Esfahani, S., 2014. Anti-inflammatory effect of *Moringa oleifera* Lam. seeds on acetic acid-induced acute colitis in rats. *Avicenna J. Phytomed.* 4, 127–136.
- Mwangi, R.W., Macharia, J.M., Wagara, I.N., Bence, R.L., 2021. The medicinal properties of *Cassia fistula* L: A review. *Biomed. Pharmacol.* 144, 112240 <https://doi.org/10.1016/j.biopha.2021.112240>.
- Nafie, M.S., Tantawy, M.A., Elmgied, G.A., 2019. Screening of different drug design tools to predict the mode of action of steroidal derivatives as anti-cancer agents. *Steroids* 152, 108485. <https://doi.org/10.1016/j.steroids.2019.108485>.
- Nagahashi, M., Shimada, Y., Ichikawa, H., Nakagawa, S., Sato, N., Kaneko, K., Homma, K., Kawasaki, T., Kodama, K., Lyle, S., Takabe, K., Wakai, T., 2017. Formalin-fixed paraffin-embedded sample conditions for deep next-generation sequencing. *J. Surg. Res.* 220, 125–132. <https://doi.org/10.1016/j.jss.2017.06.077>.
- Negm, W.A., El-Aasr, M., Attia, G., Alqahtani, M.J., Yassien, R.I., Abo Kamer, A., Elekhawey, E., 2022a. Promising antifungal activity of *Encephalartos laurentianus* de Wild against *Candida albicans* clinical isolates: *in vitro* and *in vivo* effects on renal cortex of adult albino rats. *J. Fungi*. 8 (5), 426.
- Negm, W.A., El-Kadem, A.H., Elekhawey, E., Attallah, N.G., Al-Hamoud, G.A., El-Masry, T.A., Zayed, A., 2022b. Wound-healing potential of rhoifolin-rich fraction isolated from *Sanguisorba officinalis* roots supported by enhancing re-epithelization, angiogenesis, anti-inflammatory, and antimicrobial effects. *Pharmaceuticals*. 15 (2), 178. <https://doi.org/10.3390/ph15020178>.
- Nieto, N., Torres, M.I., Fernández, M.I., Girón, M.D., Ríos, A., Suárez, M.D., Gil, A., 2000. Experimental ulcerative colitis impairs antioxidant defense system in rat intestine. *Dig. Dis. Sci.* 45, 1820–1827.
- Nishikimi, M., Roa, N., Yogi, K., 1972. Measurement of superoxide dismutase. *Biochem. Biophys. Res. Commun.* 46, 849–854.
- Nsimba, R.Y., Kikuzaki, H., Konishi, Y., 2008. Antioxidant activity of various extracts and fractions of *Chenopodium quinoa* and *Amaranthus spp.* seeds. *Food Chem.* 106 (2), 760–766. <https://doi.org/10.1016/j.foodchem.2007.06.004>.
- Obogh, G., 2005. Effect of blanching on the antioxidant properties of some tropical green leafy vegetables. *LWT—Food Sci. Technol.* 38, 513–517.
- Omer, H.A.A., Caprioli, G., Abouelenin, D., Mustafa, A.M., Uba, A.I., Ak, G., Ozturk, R. B., Zengin, G., Yagi, S., 2022. Phenolic profile, antioxidant and enzyme inhibitory activities of leaves from two *Cassia* and two *Senna* species. *Molecules* 27 (17), 5590. <https://doi.org/10.3390/molecules27175590>.
- Owusu, G., Obiri, D.D., Ainooson, G.K., Osafo, N., Antwi, A.O., Duduyemi, B.M., Anshah, C., 2020. Acetic acid-induced ulcerative colitis in Sprague Dawley rats is suppressed by hydroethanolic extract of *Cordia vignei* leaves through reduced serum levels of TNF- α and IL-6. *Intern. J. Chronic Dis.* 6, 2020.
- Paganelli, C.J., Siebert, D.A., Vitali, L., Micke, G.A., Alberton, M.D., 2020. Quantitative analysis of phenolic compounds in crude extracts of *Myrcia splendens* leaves by HPLC-ESI-MS/MS. *Rodriguésia*. 71, e00552019.
- Paglia, D.E., Valentine, W.N., 1967. Studies on the quantitative and qualitative characterization of erythrocyte glutathione peroxidase. *J. Lab. Clin. Med.* 70, 158–169.
- Pereira, P., Cebola, M.J., Oliveira, M.C., Bernardo Gil, M.G., 2017. Antioxidant capacity and identification of bioactive compounds of *Myrtus communis* L. extract obtained by ultrasound-assisted extraction. *J. Food Technol.* 54, 4362–4369.
- Pintač, D., Majkić, T., Torović, L., Orčić, D., Beara, I., Simin, N., Mimica-Dukić, N., Lesjak, M., 2018. Solvent selection for efficient extraction of bioactive compounds from grape pomace. *111Prod.* 111, 379–390.
- Popov, S.V., Markov, P.A., Nikitina, I.R., Petrishev, S., Smirnov, V., Ovodov, Y.S., 2006. Preventive effect of a pectic polysaccharide of the common cranberry *Vaccinium oxycoccos* L. on acetic acid-induced colitis in mice. *World J. Gastroenterol.* 12, 6646–6651.
- Rahmani, A.H., 2015. *Cassia fistula* Linn: Potential candidate in health management. *Pharmacol. Res.* 7, 217–224. <https://doi.org/10.4103/0974-8490.157956>.
- Saeed, N., Khan, M.R., Shabbir, M., 2012. Antioxidant activity, total phenolic and total flavonoid contents of whole plant extracts *Torilis leptophylla* L. *BMC Complementary Altern. Med.* 12, 221.
- Salama, R.M., Darwish, S.F., Shaffei, I.E., Elmongy, N.F., Afifi, M.S. and Abdel-Latif, G.A., 2020. Protective effect of *Morus macroura* Miq. fruit extract against acetic acid-induced ulcerative colitis in rats: Involvement of miRNA-223 and TNF α /NF κ B/NLRP3 inflammatory pathway. *bioRxiv*, pp.2020.12.10.1101/2020.12.22.423927.
- Sanoria, S., Qadrie, Z.L., Gautam, S.P., Barwal, A., 2020. *Cassia fistula*: Botany, phytochemistry and pharmacological leverages—a review. *Int J Pharm Pharm Sci.* 12, 90–93.
- Sarkar, S., Sengupta, A., Mukhrjee, A., Guru, A., Patil, A., Kandhare, A., Bodhankar, S., 2015. Antiulcer potential of morin in acetic acid-induced gastric ulcer via modulation of endogenous biomarkers in laboratory animals. *Pharmacologia*. 6, 273–281.
- Satheeshkumar, N., Shantikumar, S., Komali, M., 2014. Identification and quantification of aldose reductase inhibitory flavonoids in herbal formulation and extract of *Gymnema sylvestre* using HPLC-PDA and LC-MS/MS. *Chromatogr. Res. Int.* 2014.
- Shahid, M., Raish, M., Ahmad, A., Bin Jardan, Y.A., Ansari, M.A., Ahad, A., Alkharfy, K. M., Alaofi, A.L., Al-Jenoobi, F.I., 2022. Sinapic acid ameliorates acetic acid-induced ulcerative colitis in rats by suppressing inflammation, oxidative stress, and apoptosis. *Molecules* 27 (13), 4139. <https://doi.org/10.3390/molecules27134139>.
- Sharma, A., Kumar, A., Jaitak, V., 2021. Pharmacological and chemical potential of *Cassia fistula* L— a critical review. *J. Herbal Med.* 26, 100407.
- Singleton, V.L., Rossi, J.A., 1965. Colorimetry of total phenolics with phosphomolybdic-phosphotungstic acid reagents. *Am. J. Enol. Vitic.* 16, 144–158.
- Song, D.Q., Liu, J., Wang, F., Li, X.F., Liu, M.H., Zhang, Z., Cao, S.S., Jiang, X., 2021. Procyanidin B2 inhibits lipopolysaccharide-induced apoptosis by suppressing the Bcl 2/Bax and NF κ B signaling pathways in human umbilical vein endothelial cells. *Mol. Med. Rep.* 23, 267.
- Srivastava, S.K., Beutler, E., 1969. The transport of oxidized glutathione from human erythrocytes. *J. Biol. Chem.* 244, 9–16.
- Stompor-Goracy, M., 2021. The health benefits of Emodin, a Natural anthraquinone derived from Rhubarb—A Summary Update. *Int. J. Mol. Sci.* 22, 9522.
- Sun, J., Liang, F., Bin, Y., Li, P., Duan, C., 2007. Screening Non-colored Phenolics in Red Wines using liquid chromatography/ultraviolet and mass spectrometry/mass spectrometry libraries. *Molecules* 12 (3), 679–693. <https://doi.org/10.3390/12030679>.
- Sun, B., Sun, G.B., Xiao, J., Chen, R.C., Wang, X., Wu, Y., Cao, L., Yang, Z.H., Sun, X.B., 2012. Isorhamnetin inhibits H₂O₂-induced activation of the intrinsic apoptotic pathway in H9c2 cardiomyocytes through scavenging reactive oxygen species and ERK inactivation. *J. Cell. Biochem.* 113, 473–485.
- Tan, J., Zheng, M., Duan, S., Zeng, Y., Zhang, Z., Cui, Q., Zhang, J., Hong, T., Bai, J., Du, S., 2018. Chemical profiling and screening of the marker components in the fruit of *Cassia fistula* by HPLC and UHPLC/LTQ-Orbitrap MSn with chemometrics. *Molecules* 23 (7), 1501. <https://doi.org/10.3390/molecules23071501>.
- Tanideh, N., Akbari, F., Jamshidzadeh, A., Ashraf, M., Koohi-Hosseinabadi, O., Mehrabani, D., 2014. The healing effect of strawberry extract on acetic acid-induced ulcerative colitis in rat. *World Appl. Sci. J.* 31, 281–288. <https://doi.org/10.5829/idosi.wasj.2014.31.03.8355>.
- Tanideh, N., Jamshidzadeh, A., Sepehrmanesh, M., Hosseinzadeh, M., Koohi-Hosseinabadi, O., Najibi, A., Raam, M., Daneshi, S., Asadi-Yousefabad, S.L., 2016. Healing acceleration of acetic acid-induced colitis by marigold (*Calendula officinalis*) in male rats. *Saudi J Gastroenterol.* 22, 50. <https://doi.org/10.4103/1319-3767.173759>.
- Thabit, S., Handoussa, H., Roxo, M., El Sayed, N.S., de Azevedo, B.C., Wink, M., 2018. Evaluation of antioxidant and neuroprotective activities of *Cassia fistula* (L.) using the *Caenorhabditis elegans* model. *PeerJ* 6, 5159. <https://doi.org/10.7717/peerj.5159>.
- Thomas, M.J., 1995. The role of free radicals and antioxidants: how do we know that they are working? *Critical Rev. Food Sci. Nutr.* 35, 21–39. <https://doi.org/10.1080/10408399509527683>.
- Tong, L., Zhou, D., Gao, J., Zhu, Y., Sun, H., Bi, K., 2012. Simultaneous determination of naringin, hesperidin, neohesperidin, naringenin, and hesperetin of *Fractus aurantii* extract in rat plasma by liquid chromatography tandem mass spectrometry. *J. Pharm. Biomed. Anal.* 58, 58–64.
- Tsugawa, H., Nakabayashi, R., Mori, T., Yamada, Y., Takahashi, M., Rai, A., Sugiyama, R., Yamamoto, H., Nakaya, T., Yamazaki, M., Kooke, R., 2019. A cheminformatics approach to characterize metabolomes in stable-isotope-labeled organisms. *Nat. Methods* 16, 295–298.
- Vishwakarma, N., Ganeshpurkar, A., Pandey, V., Dubey, N., Bansal, D., 2015. Mesalazine-probiotics beads for acetic acid experimental colitis: formulation and characterization of a promising new therapeutic strategy for ulcerative colitis. *Drug Deliv.* 22, 94–99.
- Wang, L., Halquist, M.S., Sweet, D.H., 2013. Simultaneous determination of gallic acid and gentisic acid in organic anion transporter expressing cells by liquid chromatography-tandem mass spectrometry. *J. Chromatogr. B: Anal. Technol. Biomed. Life Sci.* 937, 91–96.
- Yang, H.Y., Wu, J., Lu, H., Cheng, M.L., Wang, B.H., Zhu, H.L., Liu, L., Xie, M., 2023. Emodin suppresses oxaliplatin-induced neuropathic pain by inhibiting COX2/NF- κ B mediated spinal inflammation. *J. Biochem. Mol. Toxicol.* 37, e23229.
- Yang, B.-Y., Zhang, X.-Y., Guan, S.-W., Hua, Z.-C., 2015. Protective effect of procyanidin B2 against CCl₄-induced acute liver injury in mice. *Molecules* 20 (7), 12250–12265. <https://doi.org/10.3390/molecules200712250>.
- Ye, M., Han, J., Chen, H., Zheng, J., Guo, D., 2007. Analysis of phenolic compounds in rhubarbs using liquid chromatography coupled with electrospray ionization mass spectrometry. *J. Am. Soc. Mass Spectrom.* 18, 82–91.
- Yen, G.C., Duh, P.D., 1994. Scavenging effect of methanolic extracts of *Peanut Hulls* on free-radical and active-oxygen species. *J. Agric. Food Chem.* 42, 629–632.
- Zabihi, M., Ahmadi, A., Zareshahi, R., 2024. Anti-inflammatory effect of aqueous extract of *Cassia fistula* in acetic acid model of colitis in rats. *J. Medicinal Plants By-product*. 2024. Jan 4.

- Zhang, Y., Pu, W., Bousquenaud, M., Cattin, S., Zanic, J., Sun, L.K., Rüegg, C., 2021. Emodin inhibits inflammation, carcinogenesis, and cancer progression in the AOM/DSS model of colitis-associated intestinal tumorigenesis. *Front. Oncol.* **10**, 564674.
- Zhong, B., Robinson, N.A., Warner, R.D., Barrow, C.J., Dunshea, F.R., Suleria, H.A.R., 2020. LC-ESI-QTOF-MS/MS characterization of seaweed phenolics and their antioxidant potential. *Mar. Drugs.* **18** (6), 331. <https://doi.org/10.3390/md18060331>.
- Zibae, E., Akaberi, M., Tayarani-Najaran, Z., Nesměrāk, K., Štícha, M., Shahraki, N., Javadi, B., Emami, S.A., 2023. Comparative LC-ESIMS-Based metabolite profiling of *Senna italica* with *Senna alexandrina* and evaluating their hepatotoxicity. *Metabolites* **13** (4), 559. <https://doi.org/10.3390/metabo13040559>.